

Strength and Microstructural Characteristics of Palm Oil Fuel Ash and Fly Ash as Binary and Ternary Blends in Self-Compacting Concrete

Brabha Hari Nagaratnam, PhD

** Corresponding Author*

Department of Mechanical & Construction Engineering

Northumbria University, Newcastle upon Tyne, NE1 8ST, United Kingdom

Email: Brabha.nagaratnam@northumbria.ac.uk

Telephone: +44(0)191 227 3496

Muhammad Abdul Mannan, PhD

Department of Civil Engineering, Faculty of Engineering, Universiti Malaysia Sarawak, 94300 Kota Samarahan, Sarawak, Malaysia

E-mail: mannan@feng.unimas.my

Muhammad Ekhlaur Rahman, PhD

School of Engineering and Science, Curtin University Sarawak, Malaysia

CDT 250 98009 Miri, Sarawak, Malaysia

Email: merahman@curtin.edu.my

Abdul Karim Mirasa, PhD

School of Engineering & Information Technology, Universiti Malaysia Sabah,

Jln UMS, 88400 Kota Kinabalu Sabah Malaysia

Email: akmirasa.ums.edu.my

Alan Richardson , PhD

Department of Mechanical & Construction Engineering

Northumbria University, Newcastle upon Tyne, NE1 8ST, United Kingdom

Email: Alan.richardson@northumbria.ac.uk

Omid Nabinejad, PhD

School of Engineering and Science, Curtin University Sarawak, Malaysia

CDT 250 98009 Miri, Sarawak, Malaysia

Email: omid.nabinejad@postgrad.curtin.edu.au

Strength and Microstructural Characteristics of Palm Oil Fuel Ash and Fly Ash as Binary and Ternary Blends in Self-Compacting Concrete

Abstract

This paper evaluates the feasibility of utilising palm oil fuel ash (POFA) and fly ash (FA) as an Ordinary Portland Cement (OPC) replacement in self-compacting concretes (SCC). The level of OPC replacement is up to 40% based on a 540 kg/m³ mix design. All concrete mixtures were restricted to the following consistency parameter; slump flow of 750 ± 100 mm, T₅₀₀ of 1.5s to 4.0s, J-Ring diameter of 650 ± 100 mm, step height of 5 to 15mm and sieve segregation resistance of less than 20%. The ternary SCC (TNY) consists of POFA and FA in equal portions. Compressive strength of SCC were determined at 7, 28 and 90 days using both cubes and cylinders. The correlation with the splitting tensile strength were evaluated. Calcium hydroxide (Ca(OH)₂) removal was measured by Differential Thermal Analysis (DTA) and its microstructural properties detected using the Scanning Electron Microscopy (SEM). When comparing the POFA and FA, it was found that the FA outperformed POFA for equal OPC replacements. In addition, the TNY blend had a marked improvement in its microstructural characteristics when compared to POFA and FA. The results also highlight that the addition of POFA and FA at higher replacement levels has significant potential for use as a medium strength concrete. Subsequently, the DTA shows that the Ca(OH)₂ for all samples with higher replacement were lower than the control at later

ages. It also demonstrated that there was a relationship between Ca(OH)_2 with regards to the compressive strength of SCC, which should be useful for forensic investigation that reveals the amount of hydrated products in concrete. Deployment of the two waste by-products of the palm oil and coal ash, would lead to a cleaner and more cost-efficient waste disposal solution for those industries, as well as advantages within the construction sector.

Keywords: binary blend; ternary blend; self-compacting concrete; microstructural properties; differential thermal analysis; scanning electron microscopy.

1. **Introduction**

Concrete is an essential material for most construction projects, it consists mainly of cement, aggregate and water. Consequently, cement is the most produced construction material with the current demand, worldwide, amounting to approximately 4 billion tonnes a year (Van Oss, 2017). For example, in Malaysia, the rapid development of infrastructure has increased the consumption of cement to 20 million tonnes annually (Bakhtyar et al., 2017). This value is expected to grow as the 11th Malaysian Plan provides more construction projects in the Sarawak state, such as additional development for the Sarawak Corridor of Renewable Energy and rural developments (Lim, 2015). This development plan is likely to have a severe environmental impact associated with a high carbon footprint. Cement production accounts to 5% of the world's carbon dioxide emissions. These rising CO_2 concentrations are likely to have profound effects on climate change (Chen et al., 2017).

Changing social needs, along with an increasing population and global traffic, produce enormous amounts of agricultural and industrial waste, annually. Some of these wastes include palm oil fuel ash (POFA), ground-granulated blast furnace slag (GGBS), rice husk ash (RHA), fly ash (FA) and silica fume (SF). Subsequently, in recent years, these waste materials have received considerable attention as a focus for research, owing to their negative impact on the quality of air, rivers, seas and groundwater, as well as, on human health (Rahman et al., 2014). Therefore, finding uses for these materials is preferable to releasing them into the environment. Thus, exploring symbiotic properties of the wastes opens new possibilities for cement development. Such type of re-used waste material, when applied as cement replacement, is known as supplementary cementitious material (SCM). It is sometimes also used as an aggregate replacement, due to its high silica content and possible pozzolanic reaction with cement (Aprianti, 2017). This type of concrete not only reduces the environmental impact of concrete production but it also affects the performance of concrete in the fresh state and with regard to strength, density or durability (Lepech et al., 2008; Kanellopoulos, 2012; Sua-iam and Makul, 2014, Khodabakhshian et al., 2018).

The continued mining or quarrying of natural aggregates, for use in concrete, eventually leads to their depletion, as well as having a huge environmental impact due to the level of emissions of CO₂ produced during their extraction (Bravo et al., 2015). Moreover, the demand for construction aggregates globally in a year is over 26.8 billion tonnes (Ashraf et al., 2013) and due to this high intensity extraction, the reuse of waste as a binder or aggregate substitute is increasing. Examples include: recycled aggregates from concrete (Dimitriou et

al., 2018), recycled construction and demolition waste (Richardson et al., 2011), tyre rubber (Mohammadinia et al., 2018) and recycled cathode ray-tube (Liu et al., 2018). Therefore, it is desirable to explore the possibilities of other materials to substitute aggregates and binders.

Sustainability issues have caused a rise in demand for concrete with varying characteristics with regard to its nature of application, such as Shotcrete, High Performance Concrete, Light Weight Concrete, Self-Compacting Concrete (SCC), Engineered Cementitious Composites, and High Strength Concrete (HSC). The focus of this research, SCC, flows through crowded reinforcement, and compacts with its own weight. This type of concrete must fulfil the passing and filling ability with sufficient segregation resistance of the mix (EFNARC, 2002). It has been observed from previous research that SCC is superior to Normally Vibrated Concrete (NVC) in a number of aspects including economical, environmental and concrete properties (Druta, 2003). In contrast with NVC, SCC is proportionally composed using less coarse aggregate and a smaller water-to-cement ratio (w/c), while a high range superplasticiser (SP) and increased volume of paste are added. This provides excellent deformability and adequate viscosity of the materials (Khayat, 1999). Despite having many advantages, there is little sign of its usage in this region. The use of POFA and FA as binary and/or ternary mixes is not common in SCC production, as there is no comprehensive study that presents the effects of using these materials.

The use of SCM, such as, metakaolin (MK), fly ash (FA), ground granulated blast furnace slag (GGBS), limestone filler (LF) and silica fume (SF) is said to enhance the fresh

properties, decrease the material cost and the amount of CO₂ produced (Almuwbbber et al., 2018; Bouzoubaa and Lachemi 2001; Mehdipour et al., 2013; Mohan and Mini, 2018; Sahmaran et al., 2011; Vejmelkova et al., 2011). One of the main types of SCM used in SCC is FA as a binary blend supplementing OPC. The benefits of incorporating FA vary on its type, proportion used, fineness, grain composition and shape, and ignition loss (Siddique and Khan 2011). As seen in the previous work by the author, Nagaratnam et al., (2016), the FA reduces the water demand of SCC and produces a liquefied consistency. Hence, an improvement was found in the passing and filling ability yet an adverse reaction was observed with regard to the segregation of the mixes. By contrast, when POFA replaced OPC it causes delays in the initial and final setting times, decreasing the passing and filling ability but enhances the consistency of the mix (segregation resistance). The benefits of adding POFA is mainly attributed to its fineness. Moreover, owing to these disparate attributes the combinations of SCM in binary and ternary blends have considerable significance in concrete technology, (Ahari et al., 2015; Gesoglu et al., 2012; Guneyisi et al., 2011; Guneyisi et al., 2010; Ismail et al., 2013; Sahmaran et al., 2006). Sahmaran et al., (2006) evaluated the compressive strength of SCC made with varying cementitious blends of FA, GGBS, and SF. They found that among all the SCM used, FA was most prominent in reducing the compressive strength of the SCCs. Furthermore, Gesoglu et al., (2012) investigated the compressive strength of SCCs with FA, marble powder (M) and limestone filler (LF). Their results found that, at an early age, the compressive strength of binary samples were higher than the ternary samples with FA. However, at later ages, there was no significant difference.

There is also other research on the positive effects of FA on compressive strength, especially at later ages, examples being combinations of: FA and recycled alumina (Sua Iam and Makul, 2017), FA and rice husk ash (Sua Iam and Makul, 2014), FA and GGBS (Su and Miao, 2003), FA and LF (Bermejo et al., 2010), FA and SF (Turk, 2012). Furthermore, others also report the effect of various SCMs on splitting tensile strength. Both Hauke (2001) and Köning et al., (2001) reported an increased value of 9.1% and 13.5% respectively in SCCs with FA, whereby Fava et al., (2003) registered an increase of 10.5% in SCCs with GGBS compared to FA. In addition, Sahmaran et al., (2009) illustrated that the tensile strength decreased as FA content increased, but improved with age. They also put forward a theory that the interfacial bond between the paste and aggregate improved in FA samples of to 50% replacement. However, to date, there is no study on the ternary blended SCC incorporating POFA and FA. The core issue with this application is the hygroscopic nature of POFA that causes an increase in water demand in SCC, which is needed for a similar workability as FA (Nagaratnam et al., 2016). On the other hand, POFA improves the segregation resistance of the SCC. As reported by the authors, the ternary blended SCC mixes not only has beneficial effects in terms of its workability properties but also lowers the amount of heat dissipation with peak temperatures occurring earlier than the other mixes.

The local construction industry in the Borneo region of Malaysia mainly consists of housing and low-rise buildings within the medium strength grade of 25 MPa to 40 MPa. In general, the concrete mix have a coarse aggregate content of about 1000 kg/m³ and the cement content is about 360 kg/m³. With its increasing development, there has been a shortage of labourers,

which has resulted in delays of various construction projects and add to the construction cost. Although it has been more than two decades since the introduction of SCC, its use in this region is merely confined to special projects, since the estimated costs are expected to be higher. In addition to that, research projects do not satisfy the main needs of the construction industry, in terms of the concrete strength, as most of the research is based on high strength SCC (Vilanova, 2009). Thus, there is still a need for further research into SCC before it can be used locally. Although SCC is not expected to ever completely replace conventional NVC, the use of the material in both the precast and ready-mix markets is expected to increase as the experience and technology improve (Goodier, 2003). Hence, the main aim of this research is to investigate the widely available POFA and FA wastes in SCC in terms of its compressive strength, tensile strength and microstructural characteristics and its suitability as medium strength concrete for the local construction industry. Thus, it is clear from the aforementioned, that there are benefits and advantages in developing SCC from blended waste materials so that lower costs and sustainability can be achieved in the construction industry.

2. Experimental Investigation

2.1 Materials

2.1.1 Cement

The Ordinary Portland Cement (OPC) of CEM 1 42.5 N (based on ASTM: C150) was used as the binder. The physical and chemical analysis of OPC is given in Table I and II, whereas the

particle size distribution, XRD (X-ray diffraction) particles and SEM imaging are shown in Figure 1, 2 and 5(a) respectively.

2.1.2 Palm Oil Fuel Ash (POFA)

The POFA were acquired from the local Sarawak Oil Palm Berhad mill. Originally, the average particle size was 100 μm but, after crushing with a ball mill, the fineness reduced to 12.9 μm (Table 1). Figure 1 further elaborates its particle size distribution. In addition, the SEM imaging (Figure 5.b), shows that the amorphous particles were irregular and angular. When viewed at a scale of 20 times larger (Figure 5.b(ii)), it appears like a honeycomb with porous microstructure.

The XRD pattern for the POFA samples is presented in Figure 3 and supports the XRF analysis (Table 2). In both analyses, the major crystalline phase was silica dioxide (SiO_2) at 57.8%. Kroehong et al., (2011) and Chandara et al., (2010) reported comparable values. However, one major difference exists between their samples and these local samples, as it also contains 20.7% graphite or carbon. Moreover, there are no ASTM chemical compositional restrictions for POFA. Here, ASTM C618 standards for FA were applied. The sum of SiO_2 , Al_2O_3 and Fe_2O_3 was 69%, which is slightly below the 70% mark for Class C pozzolans in FA.

2.1.3 Pulverised Fly Ash (FA)

The low calcium FA was collected from the Sejingkat Power Station in Malaysia. The particle size for FA is shown in Table 1 and further illustrated in Figure 1. In addition, the XRD results (Figure 4) are in line with the XRF results (Table II), with samples indicating high SiO₂ content. There are also traces of aluminium (Al₂O₃) and carbon (LOI) in the mix. Also, a study of the chemical composition indicated that the sum of SiO₂, Al₂O₃ and Fe₂O₃ was 87%, which is then more than the 70% required under Class F of the ASTM C618. Furthermore, the magnesium oxide and sulphur trioxide were well within the 5% maximum limit.

In addition, Figure 5(c) show how the locally available FA particles was mainly crystalline in form while having a smooth round surface with no air spaces. The morphology is similar to previous micrographs by Jaturapitakkul et al., (2004), Sahmaran at al., (2009), and Sharma et al., (2012).

2.1.4 Coarse Aggregates

The crushed quartzite used had a 10 mm nominal size. The physical, mechanical and chemical properties are demonstrated in Table III. Also, its particle size distribution is displayed in Figure 6. These samples are categorised as single sized aggregates.

2.1.5 Blended Fine Aggregates

Two types of aggregates were introduced after the bulk density test. As seen in Table III, the first type was crushed quartzite, or quarry dust retrieved from quarrying waste and the other type was raw river sand. Both type had a 600 μm minimum size. Since, the fineness modulus for the river sand was relatively low (1.29), hence, the coarser quarry dust (fineness modulus of 4.29) was introduced in the mix. This ratio then improved to 2.7 after blending both types of aggregates.

2.1.6 Chemical Admixture

A high range super-plasticiser (SP), Glenium Ace 389, supplied by BASF (Malaysia) was used as the chemical admixture. It falls under the type F category as per BS EN 934-2 and ASTM C494. The SP used, reduces at least 12% of the amount of water required in a mix to achieve a given mix consistency.

2.2 Mixture Proportions

In this study, the OPC, coarse aggregate, quarry dust and the sand were all kept at constant weights of 540, 400, 600 and 550 kg/m^3 , respectively. The binary and ternary replacements were made over a range of 0 to 40% (at 10% intervals) by mass of the total cementitious material. There were thirteen batches in total: a control mix (denoted C), the FA replacements (FA), the POFA replacements, and ternary blended cement replacements (TNY) which uses equal portions of POFA and FA. For all mixes, the water to binder ratio were 0.38 except for

POFA30 and POFA40, which had to be increased to 0.44. The SP content for the mixes are shown in Table IV. It is worth mentioning that the SP content was also adjusted with the purpose of maintaining high workability properties of the SCC (slump 750 ± 100 mm in addition to fulfilling passing ability and segregation resistance conditions).

2.3 Mixing Procedure

A specific mix procedure needed to be developed after various trials, as SCC mixes become more viscous as the POFA content increases. Adding water or SP sometimes led to the samples failing either all, or some, of the workability conditions. All samples were batched in a forced-action, cylindrical pan mixer, by first adding all the aggregates into it, then running this for approximately 15 mins. OPC, FA and/or POFA were then added to the aggregates and run for another 8 mins. Following that, most of the water (about 70%) mixed thru the SP was introduced gradually to the pan mixer, which was then left to mix for 3 mins more. The flow rate and consistency of the resulting mix were measured, and any remaining water needed was gradually introduced to achieve required tolerances. The resulting mix was then allowed to rest for 3 mins and remixed for another 20 to 30 secs.

2.4 Testing the Samples

2.4.1 Tests on Strength

For cylinder compressive strength (f_{cyl}) and tensile strength (f_{ct}), each mix required twelve 100 x 200 mm mould, and three cube mould of 150 mm for the cube compressive strength

(f_{cube}). It was essential to evaluate both cylinders and cubes, as in the design of civil engineering structures in Malaysia, British Standards are always applied; therefore, cubes are generally employed to measure concrete compressive strength. However, the recent move to Eurocode 2, by most countries, is based on cylinder compressive strength (Zanina, 2015). Furthermore, research work has been done in Europe to verify the average cylinder/cube strength ratio. Domone (2007) reported this to be 0.87. However, the derived results are from materials produced in Europe, while materials in South East Asia can vary significantly. The samples were cured for 7, 28 and 90 days, then tested as per ASTM C39 and BS 1881-116 guidelines for cylinders and cubes, respectively. Cylinder samples with uneven top surfaces were capped with a mix containing sulphur, as per ASTM C617.

A consistency test of cylinder compressive strength for 30 samples was also carried out to verify the variability of the mixes at 28-days in three batches; 10 samples in the morning, 10 samples in the afternoon and the rest in the evening. This is to ensure that the samples had an average compressive strength without the influence of temperature and relative humidity of the surrounding condition. SCC using 40% replacement of binary and ternary blended of POFA and FA was chosen for the consistency test as the initial tests indicated that the cylinder compressive strength to be within the target of medium strength concrete (25 to 40 MPa). Subsequently, the mean compressive strength, the standard deviation and the coefficient of variation were identified for those samples. Following on, tensile strength test were conducted as per the ASTM C496 guidelines.

2.4.2 Microstructural Analysis

For the microstructural analysis, samples were evaluated through TGA (Thermogravimetric analysis) and DTA (Differential Thermal Analysis) at 7, 28 and 90 days. Both TGA and DTA measure the temperature intervals, with corresponding reaction regions, as a function of time. After reaching their specified age, cylinders were drilled at varying position, and samples obtained were further crushed using a mortar and pestle. These samples were then passed through a 75 μ m sieve. To stop further hydration, samples were soaked in ethanol and, subsequently, oven dried at 40°C overnight. The samples were later placed under inert compressed nitrogen gas as per ASTM E1131 – 08 and heated to 1100°C. The produced DTA curve, for each sample, was then explored by monitoring step changes, occurring through moisture loss, decomposition, dehydration, and carbonation. Consequently, from the values obtained, the Ca(OH)₂ content was calculated. Furthermore, at 90 days, a laboratory microstructural inspection was carried out, with a Scanning Electron Microscope (SEM), on four samples: the Control, POFA40, FA40 and TNY40.

3.0 Experimental Results and Discussions

3.1 Compressive Strength

The cube and cylinder compressive strength of the SCC samples is shown in Figures 7 and 8. In addition, Figure 9 illustrates the cylinder to cube strength ratio found below the line presented by Domone (2007). The compressive strength improves systematically with age. Moreover, as the POFA and FA replacement increases, the binary and ternary SCC reduces

compressive strength, compared to the Control samples. Also, a close correlation is found between the cube and cylinder compressive strengths and is given by

$$f_{cyl,100} \sim 0.97997 f_{cub,150} - 7.7207 \quad (\text{Equation 1})$$

where f_{cyl} is cylinder strength and f_{cub} is cube strength.

Compared to other materials, the highest compressive strength recorded, at corresponding percentages of replacement, was in FA SCC. As can be seen in the afore-mentioned figures, samples with lower percentages of replacement, e.g. 10%, taken at 28 days, were equal or similar in strength values, but, at higher replacement values, FA proved to have 1.4 times greater compressive strength than POFA SCC. This demonstrates that POFA mixes inhibit the strength development of the hardened SCC. The main cause is due to a more porous microstructure of POFA particles (Figure 5b(ii)) causing water to occupy the empty spaces. Hence, as it evaporates leaving voids, the SCC decreases in strength. Furthermore, the strength development for binary blended SCC was slow throughout the 90 days curing period.

In the TNY samples, it was observed that as POFA volume increased, the compressive strength weakened. Furthermore, a better improvement in strength is seen in the TNY SCC compared to POFA SCC. The improved strength characteristic of TNY is owed to the synergic effect that usually occurs when a more reactive SCM, such as FA, reacts with a less reactive one, like POFA. The synergic effect is usually due to the de-flocculation of cement

particles that occurs in the presence of FA (Isaia et al., 2003). This results in a higher amount of hydrated product, consequently producing better compressive strength.

An improvement of strength is seen in all samples with SCM at later ages. This is due to the pozzolanic and micro-filler characteristics of the waste materials. From the XRF tests, it was found that the total percentages of $\text{SiO}_2 + \text{Al}_2\text{O}_3 + \text{Fe}_2\text{O}_3$ in POFA and FA were 71.4% and 86.6% (Table II), respectively. These increased compounds possibly interact with the $\text{Ca}(\text{OH})_2$ released by the OPC and forms an additional secondary binder material similar to the primary CSH. In addition, the particle size distribution designates average sizes (D_{50}) of 10 and 13 μm for POFA and FA particles, respectively. The fineness of the particles could likely increase the formation of CSH gels, due to the pozzolanic reaction, thereby causing a longer chain of polymerization.

Additionally, Figure 10 exhibits the compressive strength versus the w/c (water to cement ratio) for all three types of mixes. This correlation provides an indication of the reactivity of the SCM in equivalent w/c. It clearly shows that the FA mixes had the highest strength values when compared to POFA or TNY. This could be credited to the slower degree of pozzolanic action of FA on the hydration process. On the contrary, Narmluk and Nawa (2014) found that the mechanism of pozzolanic reaction for FA in concrete has a long dormant period up to 28 days. Fraay et al., (1989) attributes this to the un-dissolved glassy structure of the FA particles at early ages. Moreover, adding FA also gives the option to further decrease the free water content by filling the original water-filled space and decrease the Ca/Si ratio (Brandl et al.,

2010). By contrast, POFA has the opposite effect. POFA increases the water demand in SCC and, as anticipated, demonstrates lower compressive strength than in the FA samples. Furthermore, the POFA content per volume of the SCC samples was also greater at higher replacement levels, since the material has a lower specific gravity (2.3).

From these results, the incorporation of 20% or 30% FA or POFA did not show improvement of the concrete strength, in contrast to reports from some (Dinakar et al., 2013; Kroehong et al., 2011; Liu (2010); and Sata et al., 2004; but, it was in line with Guneyisi et al., (2010) and Sua-Iam and Makul (2013). Increasing SCM up to 40% continues this decrease in strength. The pozzolanic reaction of POFA seems to be low compared to other research and could be due to the high carbon content in its constituent. This is usually quantified through the LOI content in the chemical composition (XRF test) and is therefore thought to inhibit the hydration in cement, besides decreasing the workability and increasing the w/b ratio (Chusilp et al., 2009). In addition, the greater w/b ratio is required as POFA particles has an increased surface area and porous microstructure, causing further strength reduction. Yet again, FA has a smooth, sphere-shaped particles (Figure 5c(ii)) which reduces the w/b ratio, or SP content required to maintain a good consistency within the mix and, thereby, improving compressive strength.

Even though, the carbon content was significantly higher in the locally available POFA constituents, it was still possible to use it as a binary blend of up to 40% replacement and

produce a medium strength (grade 25) SCC for this region. Furthermore, if exploited as ternary blended SCC, POFA can produce SCC samples of grade 30.

3.2 Consistency Test for Cylinder Compressive Strength

The characteristic compressive strength for the SCC mixes was verified upon a 95% confidence limit (i.e. 5% defective) in the normal binomial distribution of results. As seen in Figure 11,12 and 13, the mean value observed for POFA40, FA40 and TNY40 were 25.31, 37.3 and 30.9 MPa respectively. The standard deviation were between 2 and 3, which falls under the “excellent” category as suggested by Himsworth (Gambhir, 2004). In addition, the coefficient of variance of 7 to 11% indicates that the strength results will be close to the mean value. The characteristic strength for the samples is taken as f_c and is given by the following equation

$$f_c = f_{cm} - k\alpha \quad \text{(Equation 2)}$$

where f_{cm} is the mean strength of the samples and α is the standard deviation. The k value was taken at 1.65 since there was 30 numbers of sample as per ACI Committee 214. The characteristics strength for POFA40, FA40 and TNY40 were 20.9, 37.3 and 30.9 MPa.

3.3 Splitting Tensile Strength

Figure 14 present the average splitting tensile strength of SCC containing POFA and or FA. Similar to the compressive strength results, utilisation of FA in binary blends had better splitting tensile strength than the POFA SCC. Furthermore, the TNY SCC achieved better tensile strength values than the POFA mixes but was slightly lower than the FA mixes. It

could be due to the lower CaO content in the SCM, in contrast with OPC (Table II). This produces lower amounts of CSH gel that could contribute to its tensile strength of concrete (Jalal et al., 2013). Furthermore, in POFA SCC, the aggregate–paste bond could be weaker due to the higher w/b ratios. Moreover, Roncero et al., (2002) points out that this reduction is further enhanced when poly-carboxylate type SP is used in SCC.

3.4 Tensile verses Compressive Strength of SCC

The tensile verses compressive strengths of SCC in this research (Figure 15) in a data-fitting analysis, demonstrated a power relationship and is given by;

$$f_{cu} = 11.194 f_{ct}^{0.9683} \quad \text{(Equation 3)}$$

where f_{cu} is compressive strength and f_{ct} is the splitting tensile strength.

It illuminates good correlations ($R^2 = 0.95$) between the two strength characteristics. The values are independent of both SCM content and include samples at all curing ages and compared to other research (Liu, 2010; Sukumar, 2008; and Sahmaran 2009). Liu's results are for SCC with a similar cement content and a maximum aggregate size of 20mm. Meanwhile, Sukumar's (2008) results are for a maximum aggregate size of 12mm with SCC grade 30 to 70MPa. Furthermore, it shows that the f_{ct} of 11% is within the CEB–FIB Model Code range for normal vibrated concrete. An usual range for normal vibrated concrete is within 8-14% (Kosmatka et al., 2002). Moreover, the results from this research lean towards the right bound of the CEB-FIB range, indicating less porosity. This could be due to the addition of SCM with smaller size aggregates.

3.5 TGA / DTA Analysis

Figures 16 to 21 show the TGA/DTA curves for all the SCC mixes at 7 and 90 days. It highlights the three stage step losses; that is, the dehydroxylation of water vapour at 25°C to 200°C, dehydroxylation of Ca(OH)₂ (calcium hydroxide) henceforward, simplified as CH, at 418°C to 472°C and, finally, loss due to the de-carbonation of CaCO₃ at 450°C to 850°C. The area under the curve demonstrates the amount of sample loss for each of these compounds. For all mixes, the peak melting point of the dehydroxylation was higher, and the starting and ending stage of melting occurred later for the control sample compared to the binary and ternary mixes. In addition, it is found that all samples exhibited some pozzolanic reaction as the samples indicate a lower CH content than the control sample (Table V). This could be owed to the pozzolanic action, which consumes CH to yield secondary CSH. As seen in Table II, the Calcium Oxide (CaO) content in OPC, POFA and FA were 63.2%, 3.21% and 3.28%, respectively. Increasing the SCM content, caused a decline in the total Ca²⁺ content and subsequently reduced the formation of CH. Figure 23, illustrates the correlation (R² of about 60%) amongst the compressive strength and the calculated CH content. At 7 days, the proposed equation for the CH content is:

$$CH \text{ content (\%)} = 0.0021fcu^2 - 0.112fcu + 2.935 \quad (\text{Equation 4})$$

At 90 days, the best fit the curve suggests the following equation:

$$CH \text{ content (\%)} = 0.065fcu^{0.81} \quad (\text{Equation 5})$$

where *fcu* is the compressive strength of the SCC.

The CH content in the control sample shows lower values at 90 days compared to 7 days. Darweesh and El-Suoud (2015), and Kroehong et al., (2011), comment that the CH content of Control sample should increase from 7 days to 90 days, as hydration of cement produces more CH. The varying results are most likely because of the poly-carboxylate type of SP used that slowed down the hydration of the control samples. Furthermore, the aggregate mostly consists of CaCO_3 , which could affect the mass loss of concrete in the TGA/DTA analysis, unlike cement paste analysis.

3.5 SEM Images

Figure 24 highlights that the 90 days Control sample appears denser and contains a high amount of CSH but a negligible amount of calcium hydroxide (CH) and ettringite. The fibre-like CSH gel can be clearly seen to attach itself to the surface of plate-like CH crystals, or aggregate, to form even larger crystals. In addition, Figure 25 illustrates how the POFA SCC appears to form a net-like structure and likely indicates the presence of secondary CSH. It also shows a very small amount of CH (higher brightness crystal), as evaluated in the TGA curve (small melting curve and mass loss). Moreover, the micro-image of the FA SCC (Figure 26) shows a large amount of ettringite formation, which could be attributed to the aluminum oxide (Al_2O_3) content of 20% as compared to POFA (8.9%) or OPC (5.2%) (Table II). Similarly in Figure 20, the peak drop in temperature within 105°C to 450°C shows that there is a large amount of hydrated material, such as, CSH and/or ettringite. From Figure 27, it can

be seen that the TNY40 sample forms larger pieces of CSH and ettringite. At the same time, it can be observed that those samples are more closely packed than the POFA and FA SCC. In addition, the lower aluminum oxide content in POFA reduces the formation of ettringite in TNY SCC.

Conclusions

A total of 13 different mix proportions, with binary and ternary replacement of POFA and FA, have been tested for their strength and microstructural characteristics. The succeeding conclusions are drawn:

- i. The cylinder compressive strength of all SCC mixes with similar workability conditions, decreased as the POFA and FA content increased. The compressive strength was within a 25 to 63 MPa range, at 28 days, for all grades of concrete mixes; this being appropriate for structural use.
- ii. The inclusion of blended aggregates of sand and quarry dust did not affect the compressive strength results for SCC incorporating POFA and FA. Irrespective of the low fineness modulus of the sand, the blend of smaller size aggregates with quarry dust improved the uniformity of the mix and could be implemented to produce favourable compressive strengths.
- iii. FA mixes showed the highest strength values when the equivalent w/c ratio was evaluated. In contrast, POFA mixes had the lowest. This is largely due to the total $\text{SiO}_2 + \text{Al}_2\text{O}_3 + \text{Fe}_2\text{O}_3$ content in the particles, with POFA and FA having values of 71.4% and 86.6%, respectively.
- iv. Splitting tensile strengths of concrete mixes showed a similar trend to the compressive strengths, and were within 2.44 to 5.51 MPa at 28 days. Utilisation of FA in SCC had a better influence on its tensile strength than POFA.

- v. SCC with ternary blends showed marked improvements in terms of microstructural properties, as it lowers the CH content and ettringite formation.

The utilisation of POFA and FA, at higher percentages of replacement, could have great benefit in terms of generating cost savings for the construction industry by reducing the high volume of OPC in SCC. Furthermore, if incorporated as ternary blends, it can also significantly reduce the pollution associated with having to dispose of POFA and FA and inherently reducing CO² emission, while, improving fresh and hardened properties of SCC. In conclusion, based on this study, SCC mixtures containing POFA, FA and hybrid blended aggregates, could indeed be used to produce highly workable, uniform SCC mixes that meets all strength characteristics.

References

- [1] Van Oss, H. G., 2017. Cement, in: Minerals Yearbook, edited by: USGS, United States Geological Survey.
- [2] Bakhtyar, B., Tarek Kacemi, and Md Atif Nawaz, 2017. A Review on Carbon Emissions in Malaysian Cement Industry. *International Journal of Energy Economics and Policy* 7, 3, 282-286.
- [3] Lim, A., 2015. Sarawak scores high on foreign investments, *Borneo Post*.
- [4] Chen, J., Shen, L., Song, X., Shi, Q. and Li, S., 2017. An empirical study on the CO₂ emissions in the Chinese construction industry. *Journal of Cleaner Production*, 168, pp.645-654.

- [5] Rahman, M.E., Muntohar, A.S., Pakrashi V., Nagaratnam B.H., Sujana D., 2014. Self compacting concrete from uncontrolled burning of rice husk and blended fine aggregate. *Materials and Design*, 55, 410–415
- [6] Aprianti, E., 2017. A huge number of artificial waste material can be supplementary cementitious material (SCM) for concrete production—a review part II. *Journal of Cleaner Production*, 142, 4178-4194.
- [7] Lepech, M. D., Li, V. C., Robertson, R. E., & Keoleian, G. A., 2008. Design of green engineered cementitious composites for improved sustainability. *ACI Materials Journal*, 105(6), 567-575.
- [8] Kanellopoulos, A., Petrou, M. F., & Ioannou, I., 2012. Durability performance of self-compacting concrete. *Construction and Building Materials*, 37, 320-325.
- [9] Sua-iam, Gritsada, and Natt Makul., 2014. Utilization of high volumes of unprocessed lignite-coal fly ash and rice husk ash in self-consolidating concrete." *Journal of cleaner production* 78 (): 184-194.
- [10] Khodabakhshian, Ali, Mansour Ghalehnavi, Jorge De Brito, and Elyas Asadi Shamsabadi., 2018. Durability performance of structural concrete containing silica fume and marble industry waste powder." *Journal of Cleaner Production* 170 42-60.
- [11] Bravo, M., de Brito, J., Pontes, J., & Evangelista, L., 2015. Mechanical performance of concrete made with aggregates from construction and demolition waste recycling plants. *Journal of Cleaner Production*, 99, 59-74.

- [12] Ashraf M. Wagih, Hossam Z. El-Karmoty, Magda Ebid, Samir H. Okba. 2013. Recycled construction and demolition concrete waste as aggregate for structural concrete. HBRC Journal.
- [13] Dimitriou, G., Savva, P., & Petrou, M. F. 2018. Enhancing mechanical and durability properties of recycled aggregate concrete. *Construction and Building Materials*, 158, 228-235.
- [14] Richardson, A., Coventry, K., & Bacon, J., 2011. Freeze/thaw durability of concrete with recycled demolition aggregate compared to virgin aggregate concrete. *Journal of Cleaner Production*, 19(2), 272-277.
- [15] Mohammadinia, A., Disfani, M. M., Narsilio, G. A., & Aye, L. (2018). Mechanical behaviour and load bearing mechanism of high porosity permeable pavements utilizing recycled tire aggregates. *Construction and Building Materials*, 168, 794-804.
- [16] Liu, T., Qin, S., Zou, D., & Song, W. (2018). Experimental investigation on the durability performances of concrete using cathode ray tube glass as fine aggregate under chloride ion penetration or sulfate attack. *Construction and Building Materials*, 163, 634-642.
- [17] EFNARC. 2002. *Specification and Guidelines for Self-Compacting Concrete*.
- [18] Druta, C., 2003. *Tensile strength and bonding characteristics of SCC*. Master of Science in Engineering. Louisiana State University.
- [19] Khayat, K., 1999. Workability, testing, and performance of self-consolidating concrete. *ACI Materials Journal*, 96(3).

[20] Almuwbber, O., Haldenwang, R., Mbasha, W., & Masalova, I. 2018. The influence of variation in cement characteristics on workability and strength of SCC with fly ash and slag additions. *Construction and Building Materials*, 160, 258-267.

[21] Bouzoubaa, N., & Lachemi, M., 2001. Self-compacting concrete incorporating high volumes of class F fly ash: Preliminary results. *Cement and Concrete Research*, 31(3), 413-420.

[22] Mehdipour, I., Razzaghi, M. S., Amini, K., & Shekarchi, M., 2013. Effect of mineral admixtures on fluidity and stability of self-consolidating mortar subjected to prolonged mixing time. *Construction and Building Materials*, 40, 1029-1037.

[23] Mohan, A., & Mini, K. M. 2018. Strength and durability studies of SCC incorporating silica fume and ultra fine GGBS. *Construction and Building Materials*, 171, 919-928.

[24] Şahmaran, M., Özbay, E., Yücel, H. E., Lachemi, M., & Li, V. C., 2011. Effect of fly ash and PVA fiber on microstructural damage and residual properties of engineered cementitious composites exposed to high temperatures. *Journal of Materials in Civil Engineering*, 23(12), 1735-1745.

[25] Vejmelkova, E., Keppert, M., Grzeszczyk, S., Skalinski, B., & Cerny, R., 2011. Properties of self-compacting concrete mixtures containing metakaolin and blast furnace slag. *Construction and Building Materials*, 25(3), 1325-1331.

[26] Siddique, R., & Khan, M. I., 2011. *Supplementary cementing materials*: Springer Science & Business Media.

[27] Nagaratnam, B. H., Rahman, M. E., Mirasa, A. K., Mannan, M. A., & Lame, S. O., 2016. Workability and heat of hydration of self-compacting concrete incorporating agro-industrial waste. *Journal of Cleaner Production*, 112, 882-894.

[28] Vilanova, A. (2009). Influencia de la dosificación y empleo de diferentes tipos de cemento y adiciones en las propiedades mecánicas del Hormigón Autocompactante. PhD. Spain: Universidad Politécnica de Madrid.

[29] Goodier, C. I. (2003). Development of self-compacting concrete. Paper presented at the Proceedings of the ICE-Structures and Buildings.

[30] Ahari, R. S., Erdem, T. K., & Ramyar, K., 2015. Effect of various supplementary cementitious materials on rheological properties of self-consolidating concrete. *Construction and Building Materials*, 75, 89-98.

[31] Gesoğlu, M., Güneyisi, E., Kocabağ, M. E., Bayram, V., & Mermerdaş, K., 2012. Fresh and hardened characteristics of self compacting concretes made with combined use of marble powder, limestone filler, and fly ash. *Construction and Building Materials*, 37, 160-170.

[32] Guneyisi, E., Gesoglu, M., & Ozbay, E., 2010. Strength and drying shrinkage properties of self-compacting concretes incorporating multi-system blended mineral admixtures. *Construction and Building Materials*, 24(10), 1878-1887.

[33] Guneyisi, E., Gesoglu, M., & Ozbay, E., 2011. Permeation properties of self-consolidating concretes with mineral admixtures. *ACI Materials Journal*, 108(2), 150-158.

[34] Ismail, M., Hassan, I., Abdulrahman, A., Forouzani, P., Norizman, A., & Yusuf, T., 2013. Effect of micro-structure and mineralogical composition on the water demand and

super-plasticiser content of ternary blended self-consolidating paste. Paper presented at the Proceedings of the Thirteenth East Asia-Pacific Conference on Structural Engineering and Construction (EASEC-13).

[35] Şahmaran, M., Christianto, H. A., & Yaman, İ. Ö., 2006. The effect of chemical admixtures and mineral additives on the properties of self-compacting mortars. *Cement and Concrete Composites*, 28(5), 432-440.

[36] Sua Iam, Gritsada, and Natt Makul., 2017. Incorporation of high-volume fly ash waste and high-volume recycled alumina waste in the production of self-consolidating concrete. *Journal of Cleaner Production*, 159, 194-206.

[37] Su, N., & Miao, B., 2003. A new method for the mix design of medium strength flowing concrete with low cement content. *Cement and Concrete Composites*, 25(2), 215-222.

[38] Bermejo Núñez, E. B., Gálvez Ruíz, J., Fernández Cánovas, M., & Moragues Terrades, A., 2010. Influence of the mineral admixture on the durability of medium-strength self compacting concrete.

[39] Turk, K., 2012. Viscosity and hardened properties of self-compacting mortars with binary and ternary cementitious blends of fly ash and silica fume. *Construction and Building Materials*, 37, 326-334.

[40] Köning, G., Holsechemacher, K., Dehn, F., & Weie, D., 2001. Self-compacting concrete-time development of material properties and bond behaviour. Paper presented at the Proceedings of the 2nd international RILEM symposium on self-compacting concrete. Tokyo: COMS Engineering Corporation.

[41] Hauke, B., 2001. Self-compacting concrete for precast concrete products in Germany. Paper presented at the Proceedings of the 2nd international RILEM symposium on self-compacting concrete. Tokyo: COMS Engineering Corporation.

[42] Fava, C., Bergol, L., Fornasier, G., Giangrasso, F., & Rocco, C., 2003. Fracture behaviour of self-compacting concrete. Paper presented at the Proceedings of the 3rd international RILEM symposium on self-compacting concrete. Reykjavik: RILEM Publications SARL.

[43] Şahmaran, M., Yaman, İ. Ö., & Tokyay, M., 2009. Transport and mechanical properties of self consolidating concrete with high volume fly ash. *Cement and Concrete Composites*, 31(2), 99-106.

[44] ASTM C150. 2012. Standard Specification of Portland Cement. ASTM International West Conshohocken, PA.

[45] Chandara, C., Sakai, E., Azizli, K. A. M., Ahmad, Z. A., & Hashim, S. F. S., 2010. The effect of unburned carbon in palm oil fuel ash on fluidity of cement pastes containing superplasticizer. *Construction and Building Materials*, 24(9), 1590-1593.

[46] ASTM C618. 2015. Standard Specification for Coal Fly Ash and Raw or Calcined Natural Pozzolan for use as a Mineral Admixture in Portland Cement Concrete. ASTM International, West Conshohocken, PA.

[47] Kroehong, W., Sinsiri, T., Jaturapitakkul, C., & Chindaprasirt, P., 2011. Effect of palm oil fuel ash fineness on the microstructure of blended cement paste. *Construction and Building Materials*, 25(11), 4095-4104.

[48] Jaturapitakkul, C., Kiattikomol, K., Sata, V., & Leekeeratikul, T., 2004. Use of ground coarse fly ash as a replacement of condensed silica fume in producing high-strength concrete. *Cement and Concrete Research*, 34(4), 549-555.

[49] Sharma, A., Srivastava, K., Devra, V., & Rani, A., 2012. Modification in properties of fly ash through mechanical and chemical activation. *Am Chem Sci J*, 2(4), 177-187.

[50] ASTM C494/C494M. 2015. Admixture, W.-R. Type B (Vol. 3). ASTM International West Conshohocken, PA.

[51] Zanina, P., 2015. No turning back in Accepting New Design Structures For Earthquake Resistance. *Jurutera*.

[52] Domone, P., 2007. A review of the hardened mechanical properties of self-compacting concrete. *Cement and Concrete Composites*, 29(1), 1-12.

[53] BS EN 934-2. 2001. Admixtures for concrete, mortar and grout. *Concrete admixtures. Definitions, requirements, conformity, marking and labelling*.

[54] ASTM C39M. 2012. Standard test method for compressive strength of cylindrical concrete specimens. ASTM International, West Conshohocken, PA.

[55] ASTM C617. 1998. Standard Practice for Capping Cylindrical Concrete Specimens. ASTM International West Conshohocken, PA.

[56] ASTM C496/C496M. 2011. Standard test method for splitting tensile strength of cylindrical concrete. ASTM International West Conshohocken, PA.

[57] ASTM E1131 – 08. 2014. Standard Test Method for Compositional Analysis by Thermogravimetry. ASTM International West Conshohocken, PA.

[58] Isaia, G. C., Gastaldini, A. L. G., & Moraes, R., 2003. Physical and pozzolanic action of mineral additions on the mechanical strength of high-performance concrete. *Cement and Concrete Composites*, 25(1), 69-76.

[59] Narmluk, M., & Nawa, T., 2014. Effect of Curing Temperature on Pozzolanic Reaction of Fly Ash in Blended Cement Paste. *International Journal of Chemical Engineering and Applications*, 5(1), 31.

[60] Brandl, A., Bray, W., & Doherty, D.R., 2010. Technically and economically improved cementing system with sustainable components. Paper presented at the IADC/SPE Asia Pacific Drilling Technology Conference and Exhibition.

[61] Dinakar, P., Reddy, M.K., & Sharma, M., 2013. Behaviour of self compacting concrete using Portland pozzolana cement with different levels of fly ash. *Materials & Design*, 46, 609-616.

[62] Liu, M., 2010. Self-compacting concrete with different levels of pulverized fuel ash. *Construction and Building Materials*, 24(7), 1245-1252.

[63] Sata, V., Jaturapitakkul, C., & Kiattikomol, K., 2004. Utilization of palm oil fuel ash in high-strength concrete. *Journal of Materials in Civil Engineering*, 16(6), 623-628.

[64] Chusilp, N., Jaturapitakkul, C., & Kiattikomol, K., 2009. Effects of LOI of ground bagasse ash on the compressive strength and sulfate resistance of mortars. *Construction and Building Materials*, 23(12), 3523-3531.

[65] Gambhir, M. L. (2004). *Concrete technology*: Tata McGraw-Hill Education.

[66] Roncero, J., Valls, S., & Gettu, R., 2002. Study of the influence of superplasticizers on the hydration of cement paste using nuclear magnetic resonance and X-ray diffraction techniques. *Cement and Concrete Research*, 32(1), 103-108.

[67] Jalal, M., Ramezani-pour, A. A., & Pool, M. K., 2013. Split tensile strength of binary blended self compacting concrete containing low volume fly ash and TiO₂ nanoparticles. *Composites Part B: Engineering*, 55, 324-337.

[68] Sukumar, B., Nagamani, K., & Raghavan, R. S., 2008. Evaluation of strength at early ages of self-compacting concrete with high volume fly ash. *Construction and Building Materials*, 22(7), 1394-1401.

[69] Kosmatka, S., Kerkhoff, B., Panarese, W., MacLeod, N., & McGrath, R., 2002. *Design and Control of Mixtures: Vol. Engineering Bulletin*.

[70] Darweesh, H.H.M., and Abo-El-Suoud M.R., 2015. Quaternary Cement Composites Containing Some Industrial By-products. *Chemistry*.

List of Tables:

Table I: Physical composition of OPC, POFA and FA

Table II: Chemical composition of OPC, POFA and FA

Table III: Physical, mechanical and chemical properties of aggregates

Table IV: Mix proportions

Table V: CA(OH)₂ content of samples

List of Figures:

Figure 1: Particle size distribution of OPC, POFA, FA and blended POFA and FA.

Figure 2: XRD of OPC particles

Figure 3: XRD of POFA particles

Figure 4: XRD of FA particles

Figure 5: SEM imaging for; (a) OPC (b) POFA and (c) FA at (i) at 100x μm and (ii) 20x μm

Figure 6: Particle size distribution of aggregates

Figure 7: Cylinder compressive strength of SCC incorporating blended POFA and FA

Figure 8: Cube compressive strength of SCC incorporating blended POFA and FA

Figure 9: Cube compressive strength vs. cylinder to cube compressive strength ratio

Figure 10: Relationship between compressive strength and water to cement ratio of SCC using POFA, FA and TNY

Figure 11: Normal distribution function for SCC using POFA40

Figure 12: Normal distribution function for SCC using FA40

Figure 13: Normal distribution function for SCC using TNY40

Figure 14: Splitting tensile strength for SCC incorporating blended POFA and FA

Figure 15: Splitting tensile strength vs. compressive strength

Figure 16: TGA/DTA Curve of Control and POFA SCC at 7 Days

Figure 17: TGA/DTA Curve of Control and FA SCC at 7 Days

Figure 18: TGA/DTA Curve of Control and TNY SCC at 7 Days

Figure 19: TGA/DTA Curve of Control and POFA SCC at 90 Days

Figure 20: TGA/DTA Curve of Control and FA SCC at 90 Days

Figure 21: TGA/DTA Curve of Control and TNY SCC at 90 Days

Figure 22: $\text{Ca}(\text{OH})_2$ Content of samples through Thermogravimetric Analysis

Figure 23.: Relationship between $\text{Ca}(\text{OH})_2$ content and Compressive Strength at 7 and 90 days

Figure 24: SEM Image for Control SCC at 90 days

Figure 25: SEM Image for POFA40 at 90 days

Figure 26: SEM Images for FA40 at 90 days

Figure 27: SEM Image for TNY40 at 90 days

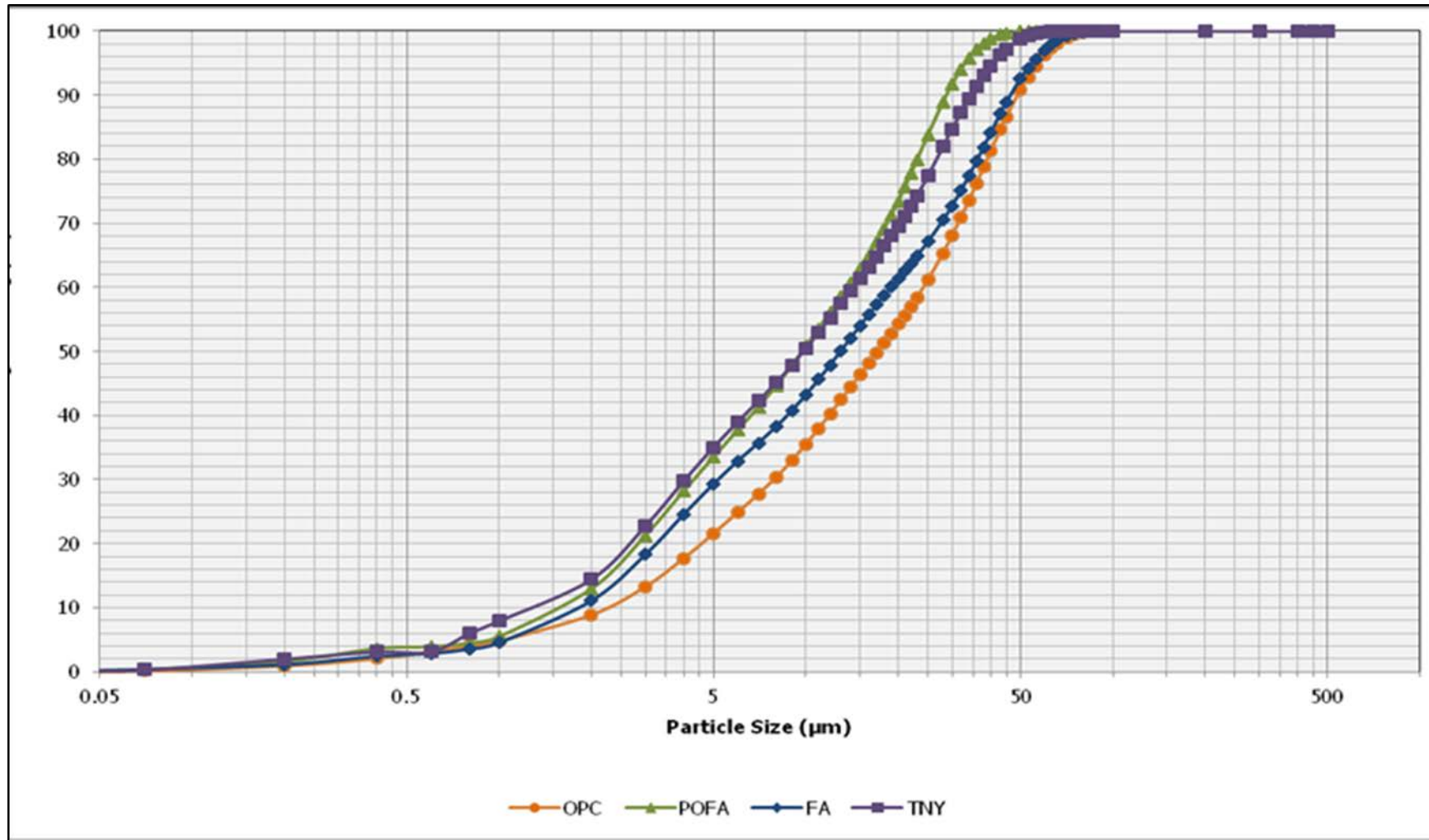


Figure 1: Particle size distribution of OPC, POFA, FA and blended POFA and FA (TNY)

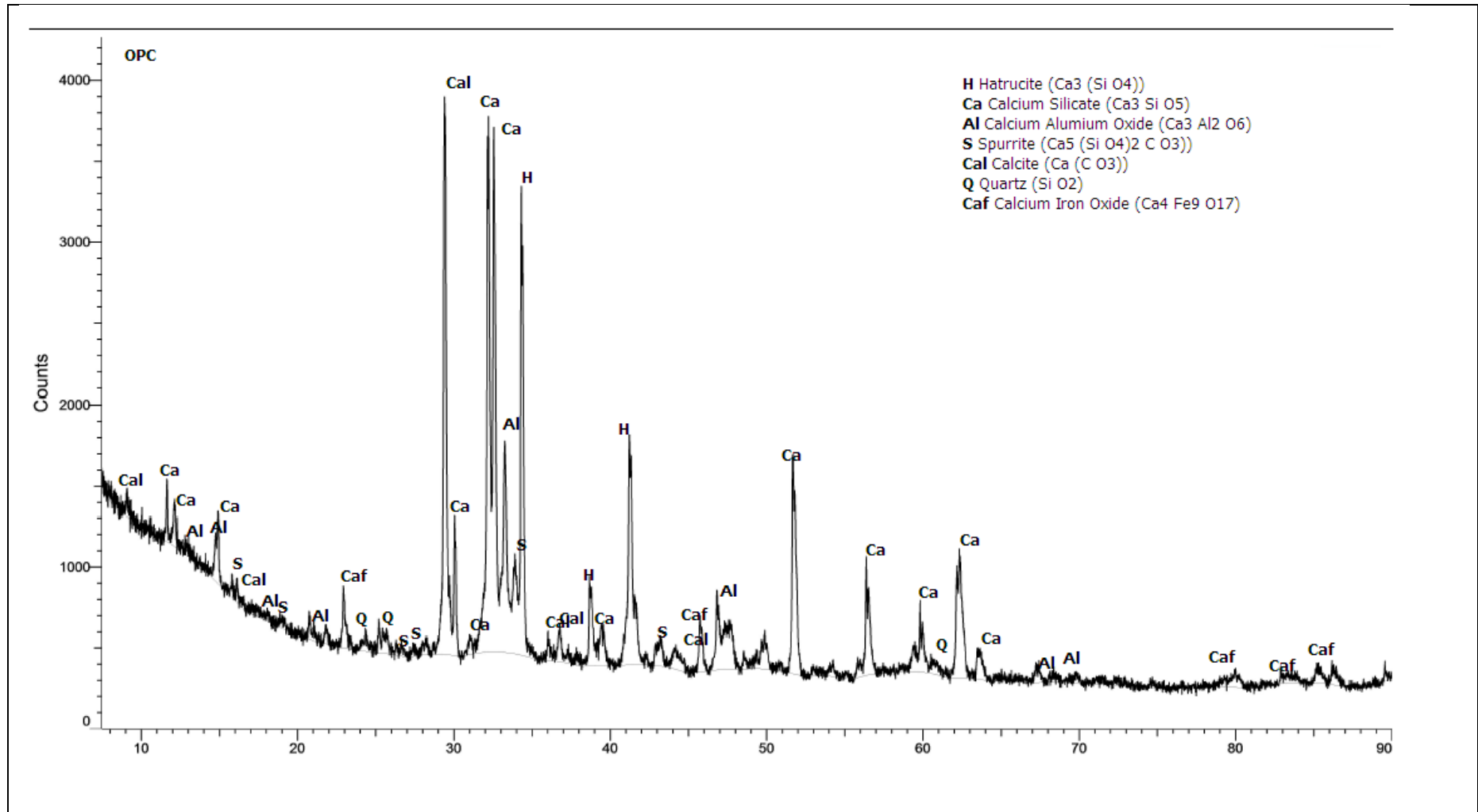


Figure 2: XRD of OPC particles

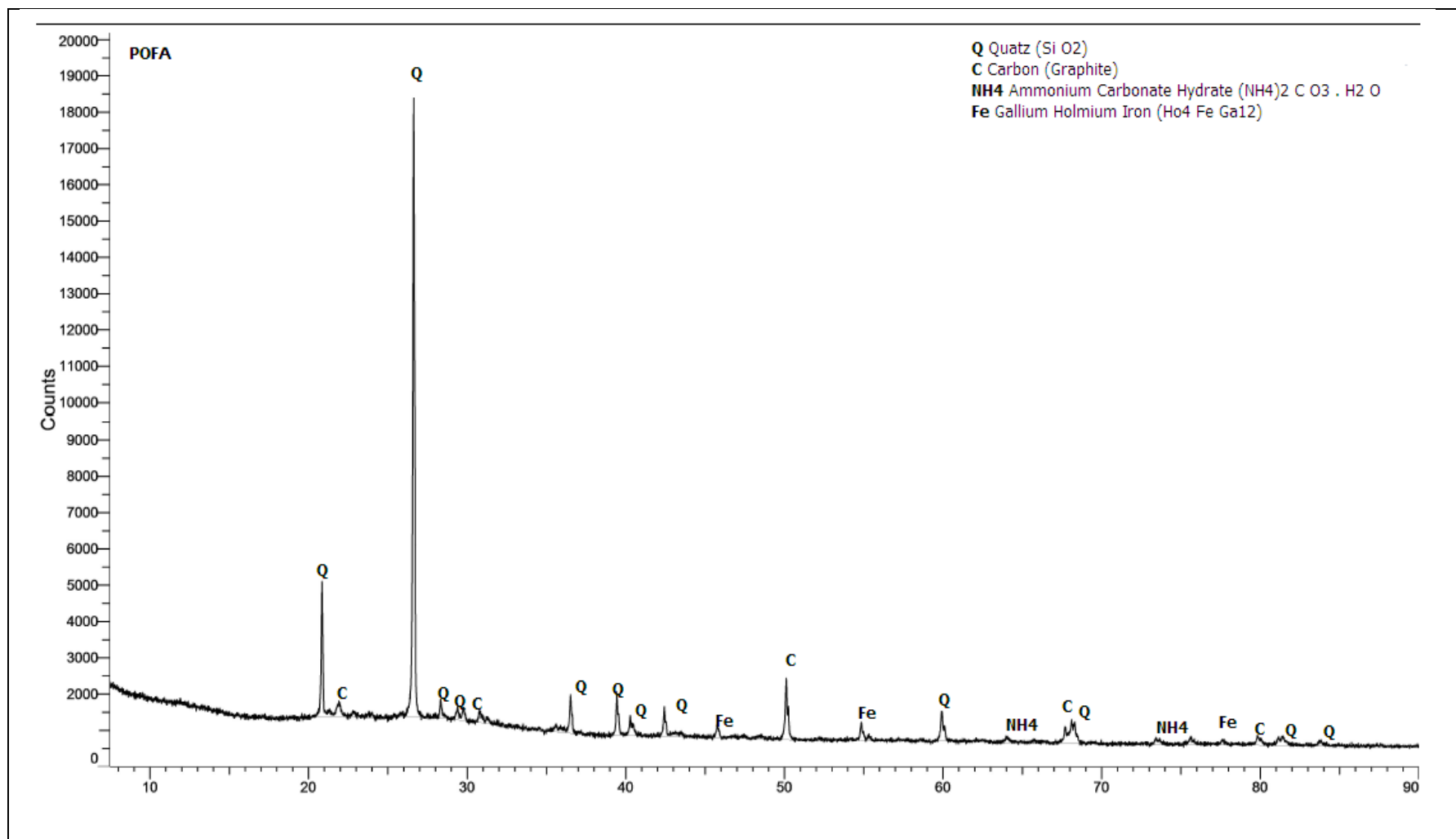


Figure 3: XRD of POFA particles

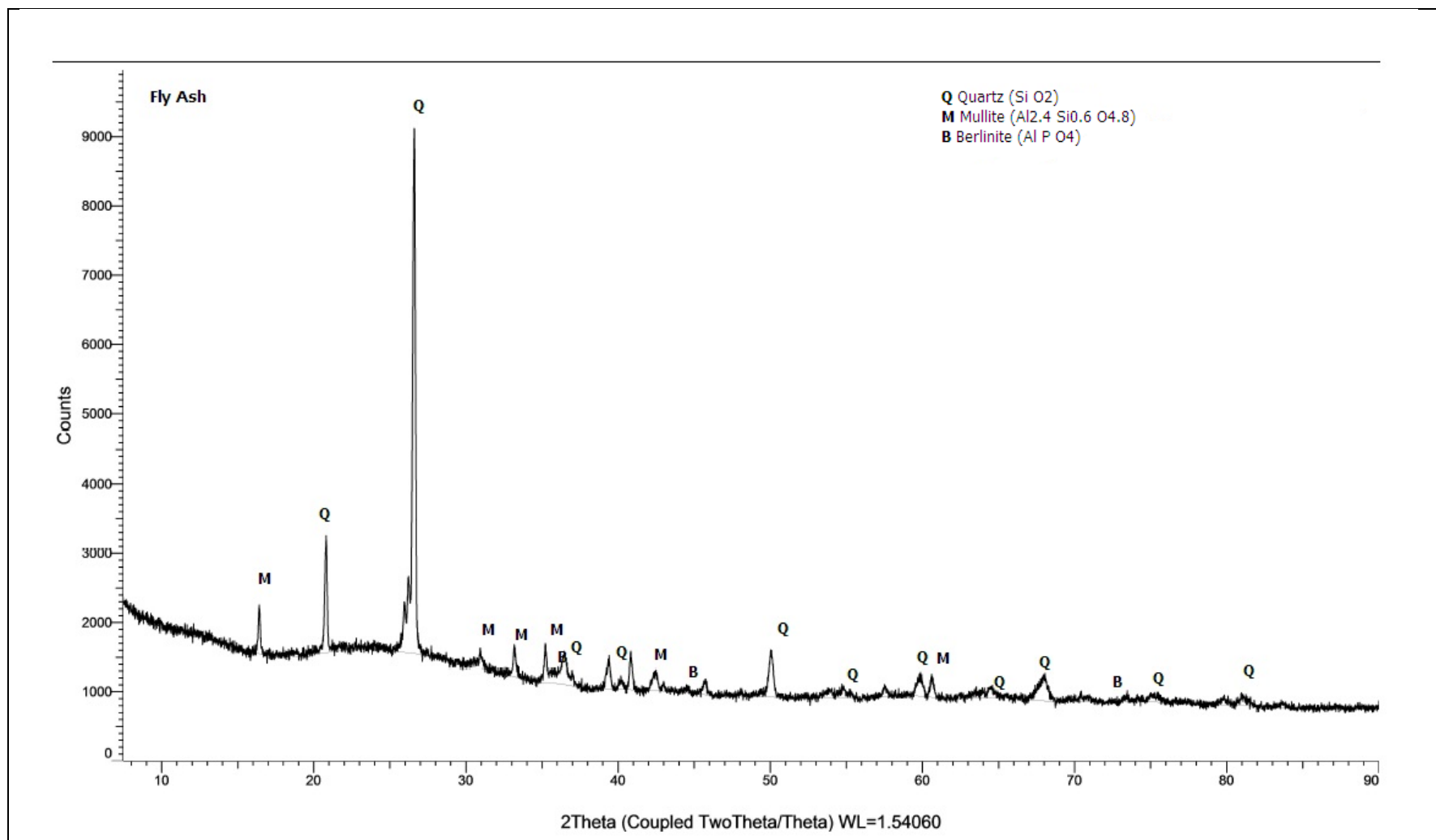


Figure 4: XRD of FA particle

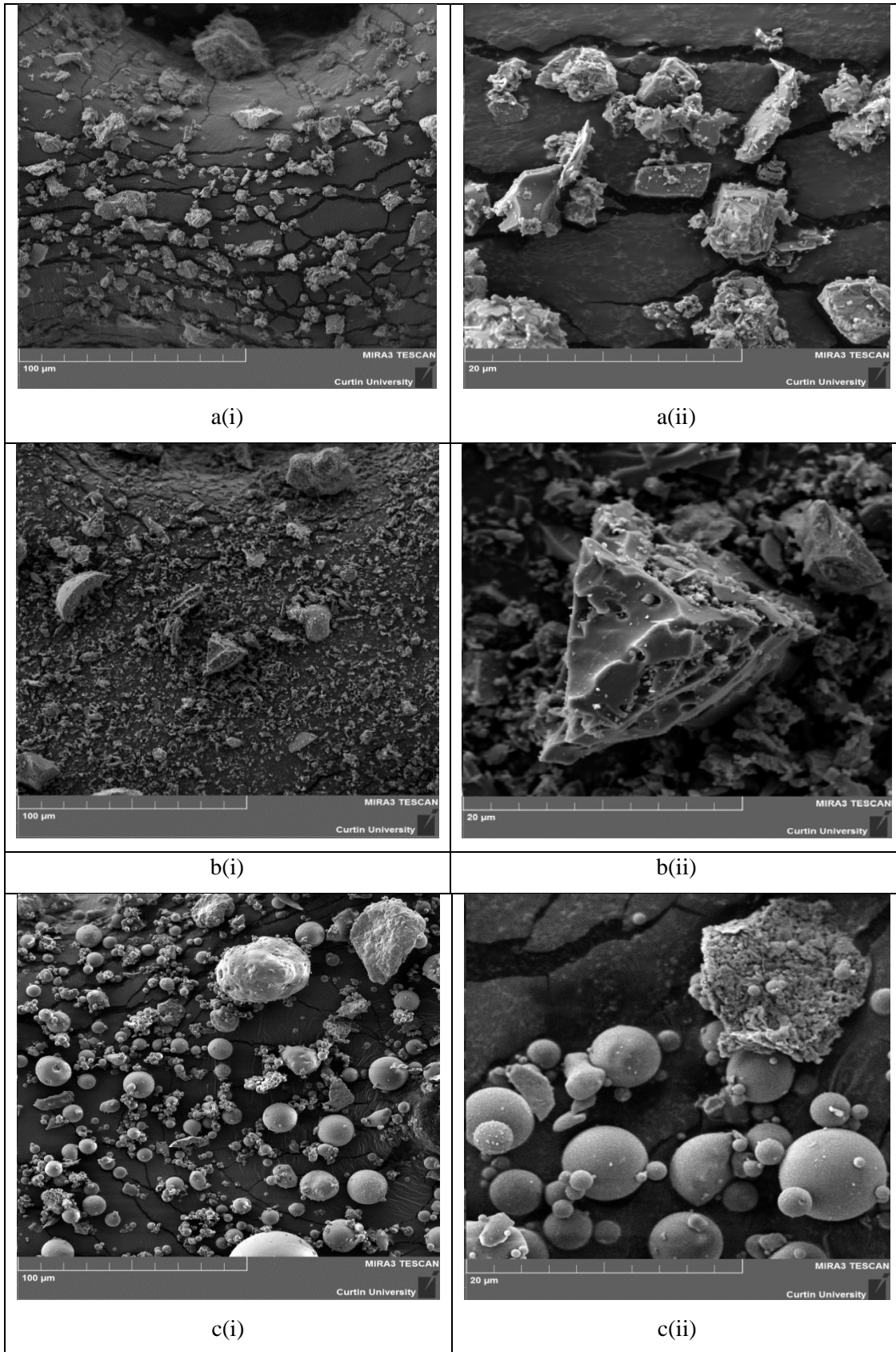


Figure 5: SEM imaging for; (a) OPC (b) POFA and (c) FA at (i) at 100x μm and (ii) 20x μm

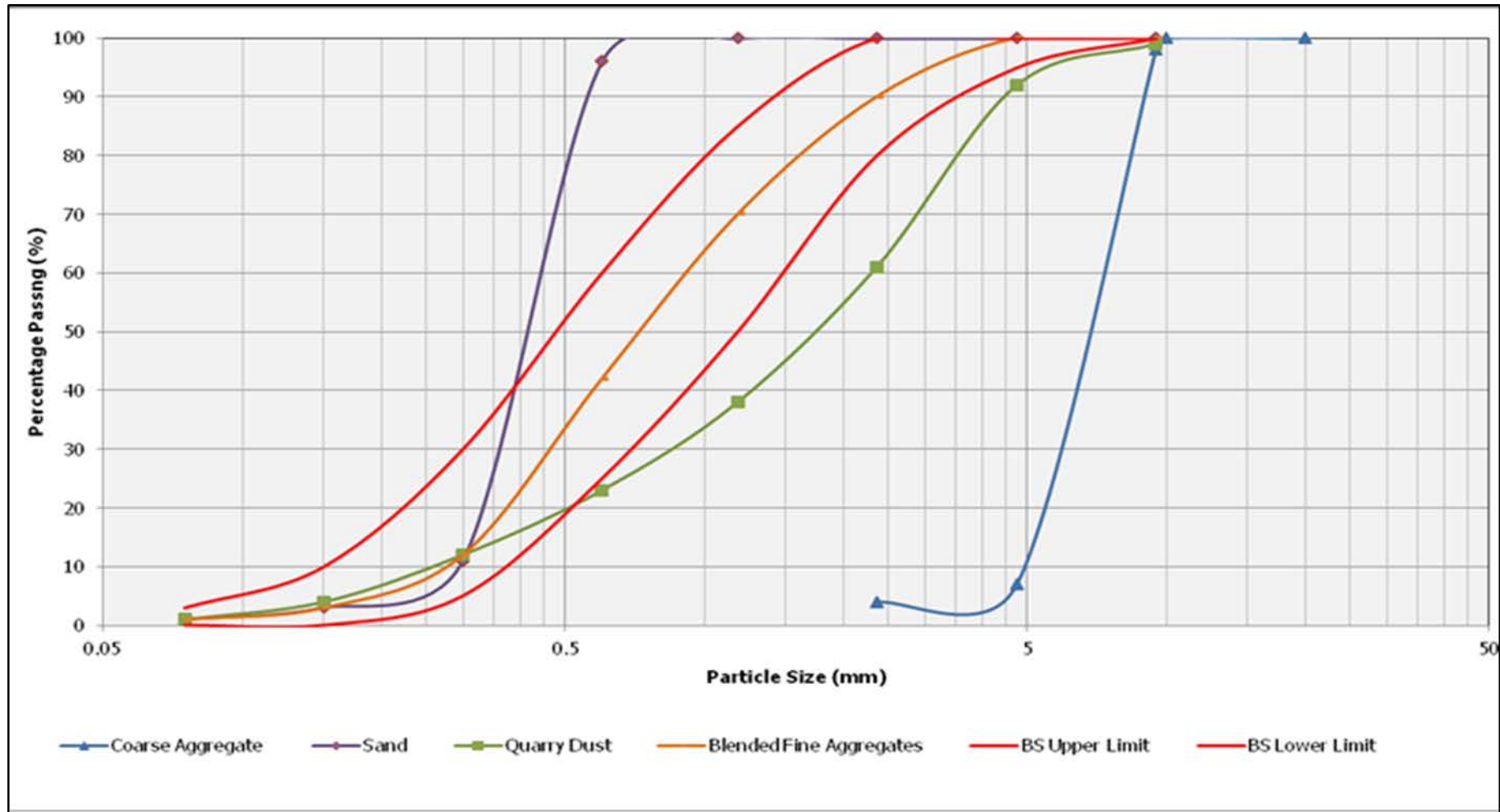


Figure 6: Particle size distribution of aggregates

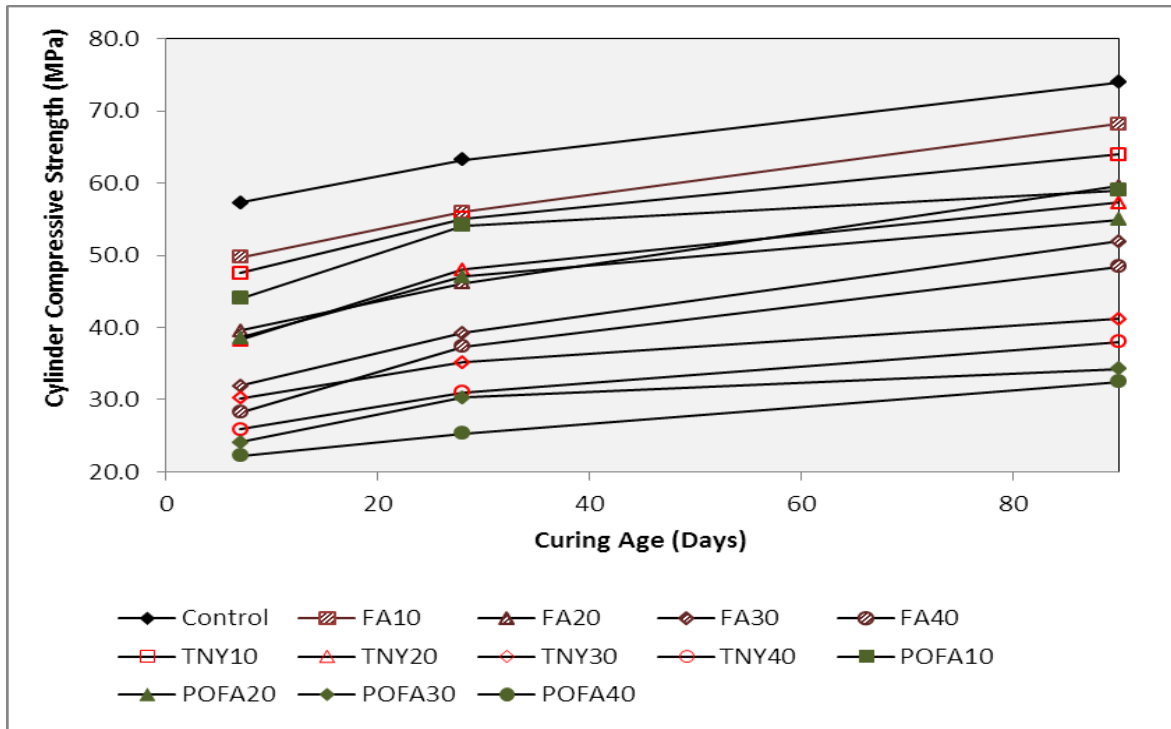


Figure 7: Cylinder compressive strength of SCC incorporating blended POFA and FA

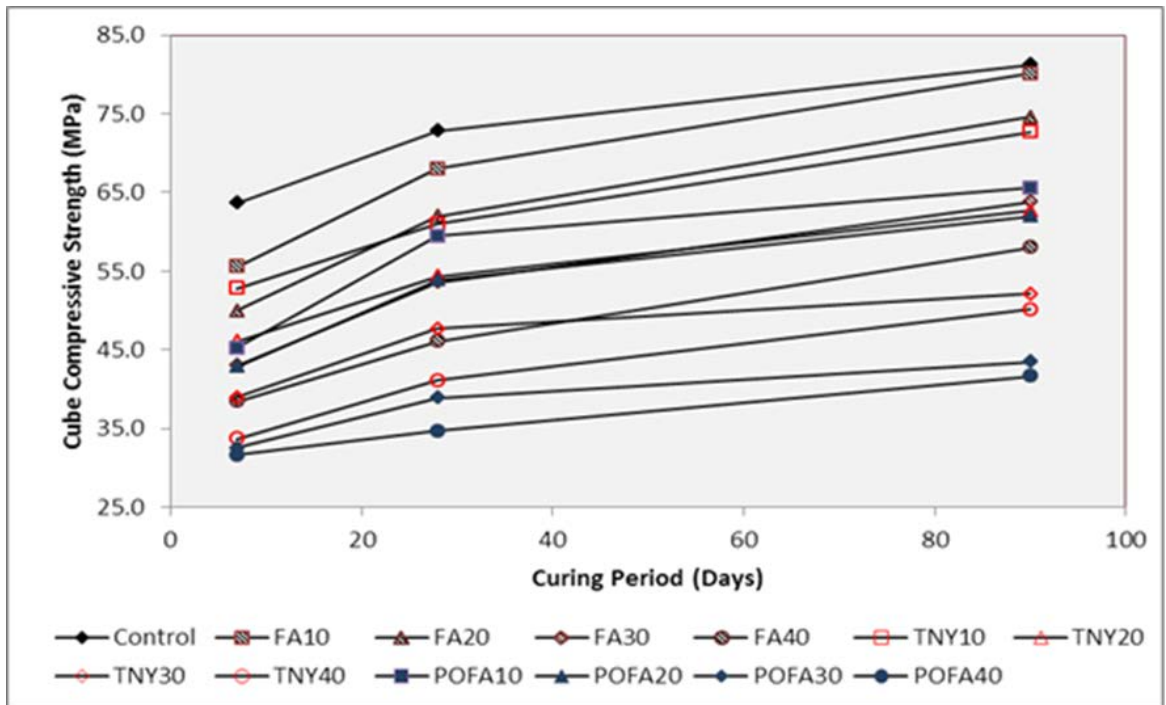


Figure 8: Cube compressive strength of SCC incorporating blended POFA and FA

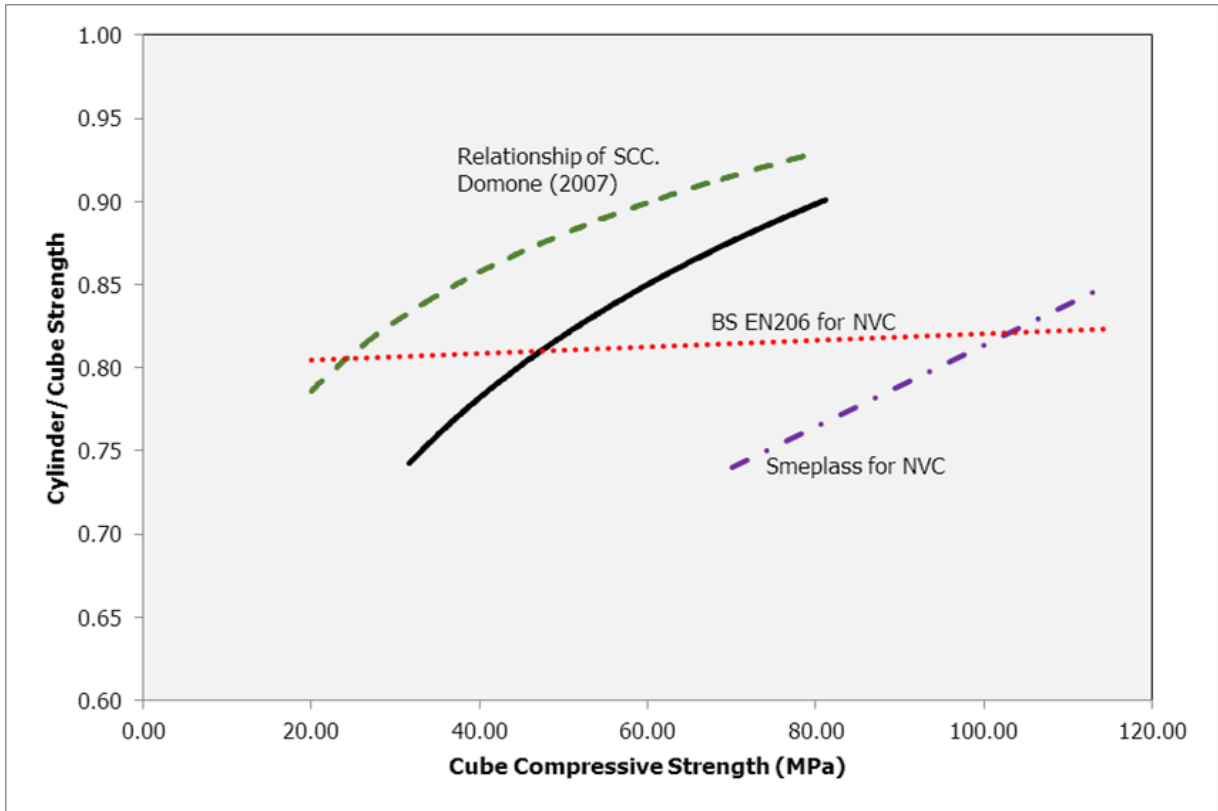


Figure 9: Cube compressive strength vs. cylinder to cube compressive strength ratio

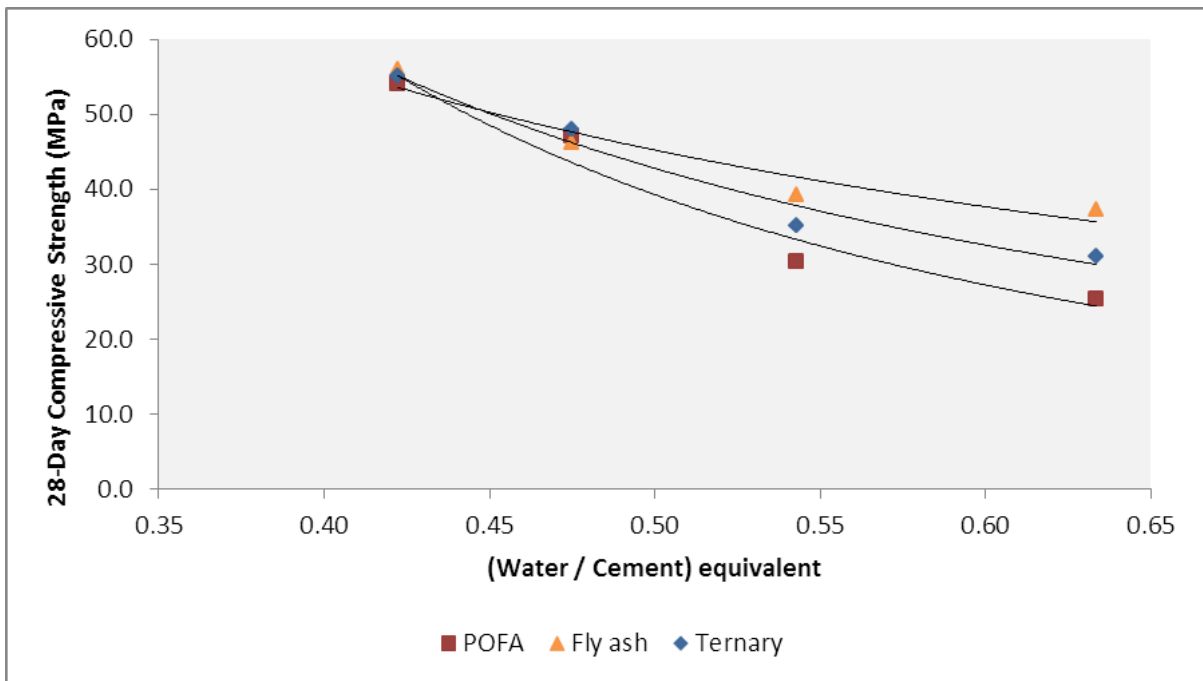


Figure 10: Relationship between compressive strength and w/c ratio of SCC using POFA, FA and TNY

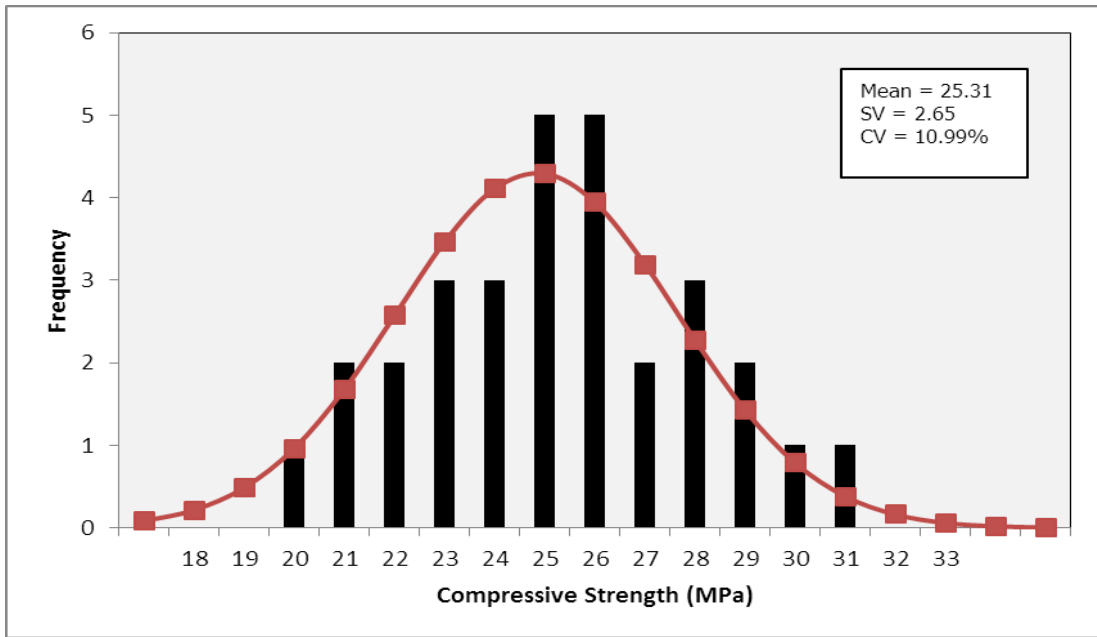


Figure 11: Normal distribution function for SCC using POFA40

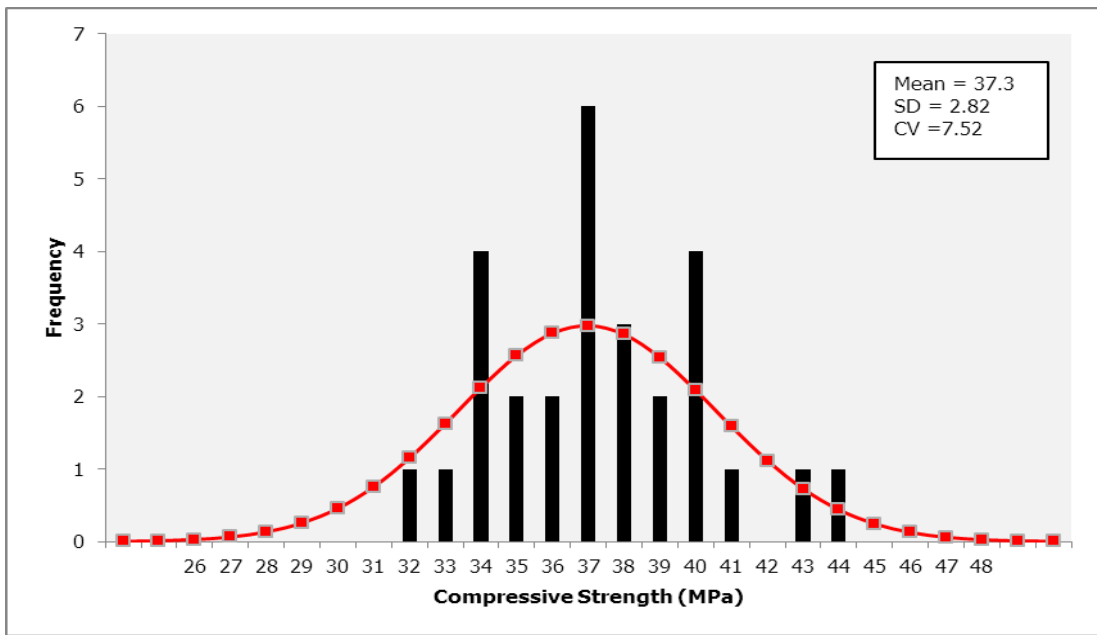


Figure 12: Normal distribution function for SCC using FA40

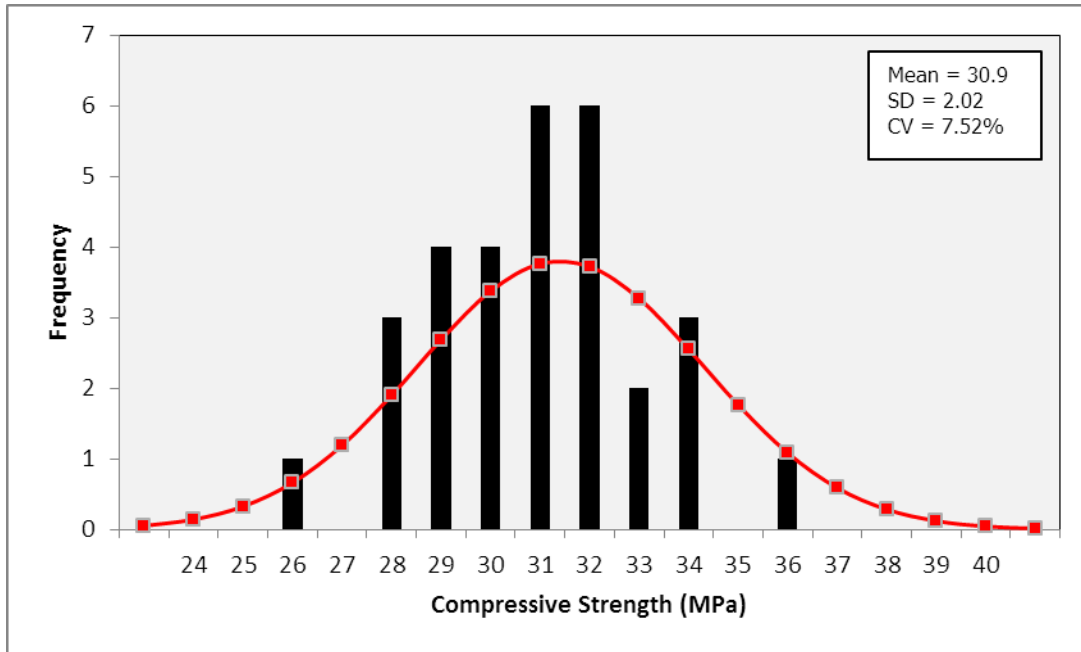


Figure 13: Normal distribution function for SCC using TNY40

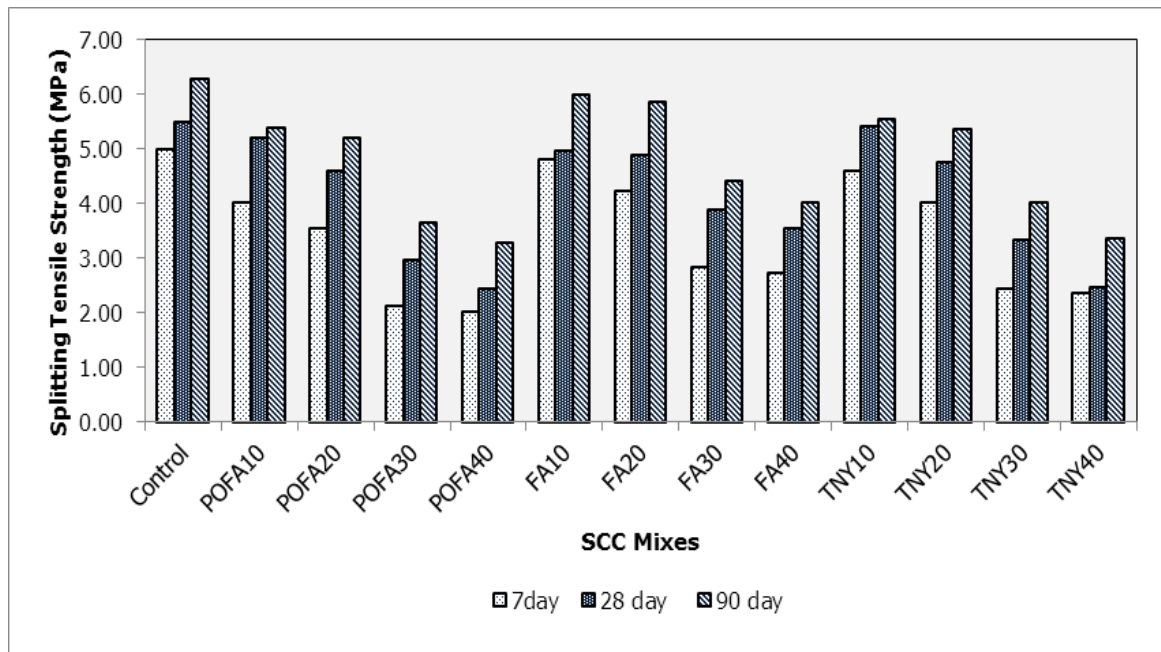


Figure 14: Splitting tensile strength for SCC incorporating blended POFA and FA

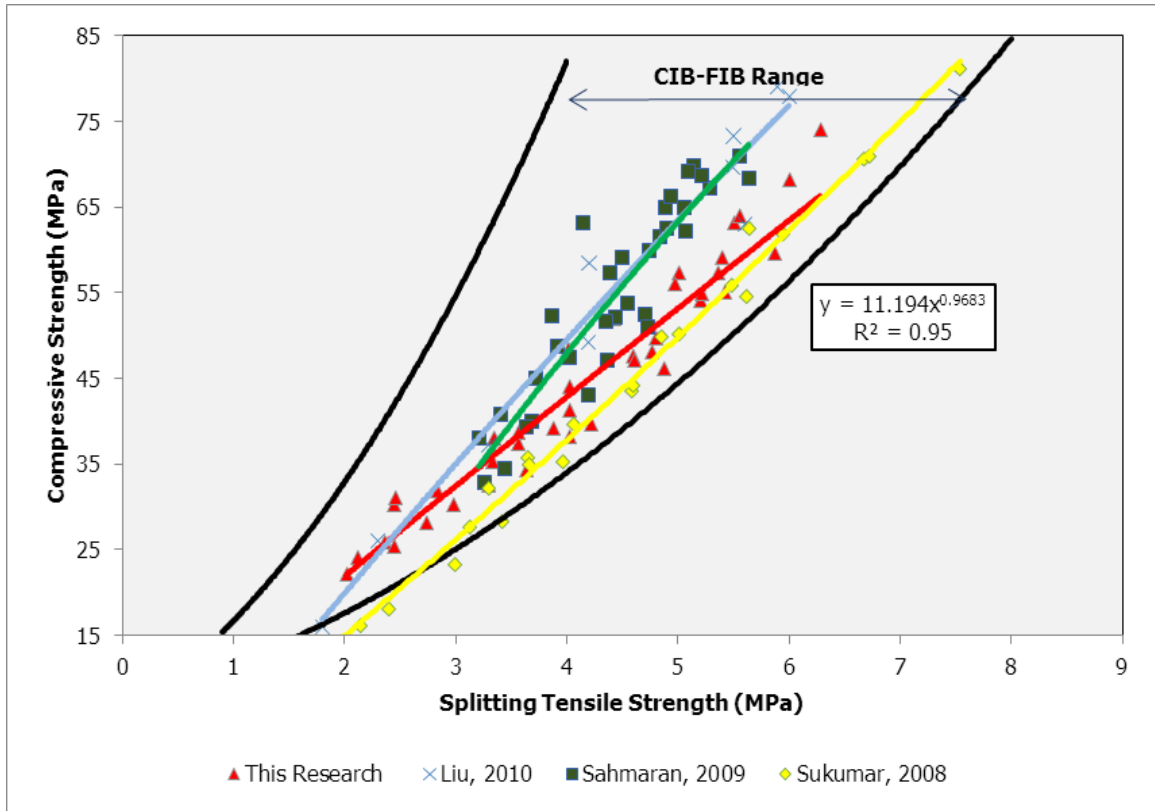
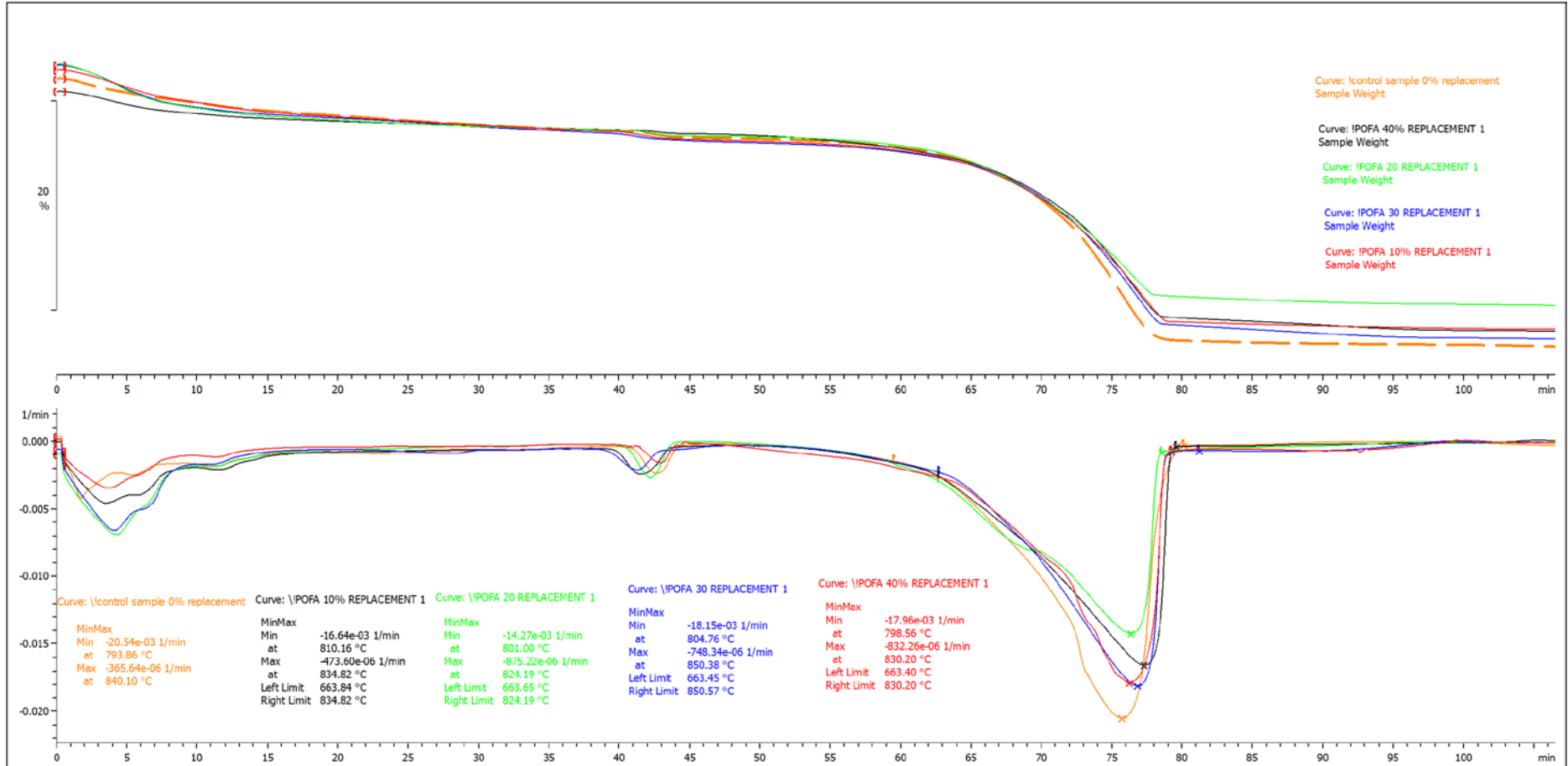


Figure 15: Splitting tensile strength vs. compressive strength

^exo

7 days POFA

28.08.2016 23:46:46



METTLER TOLEDO

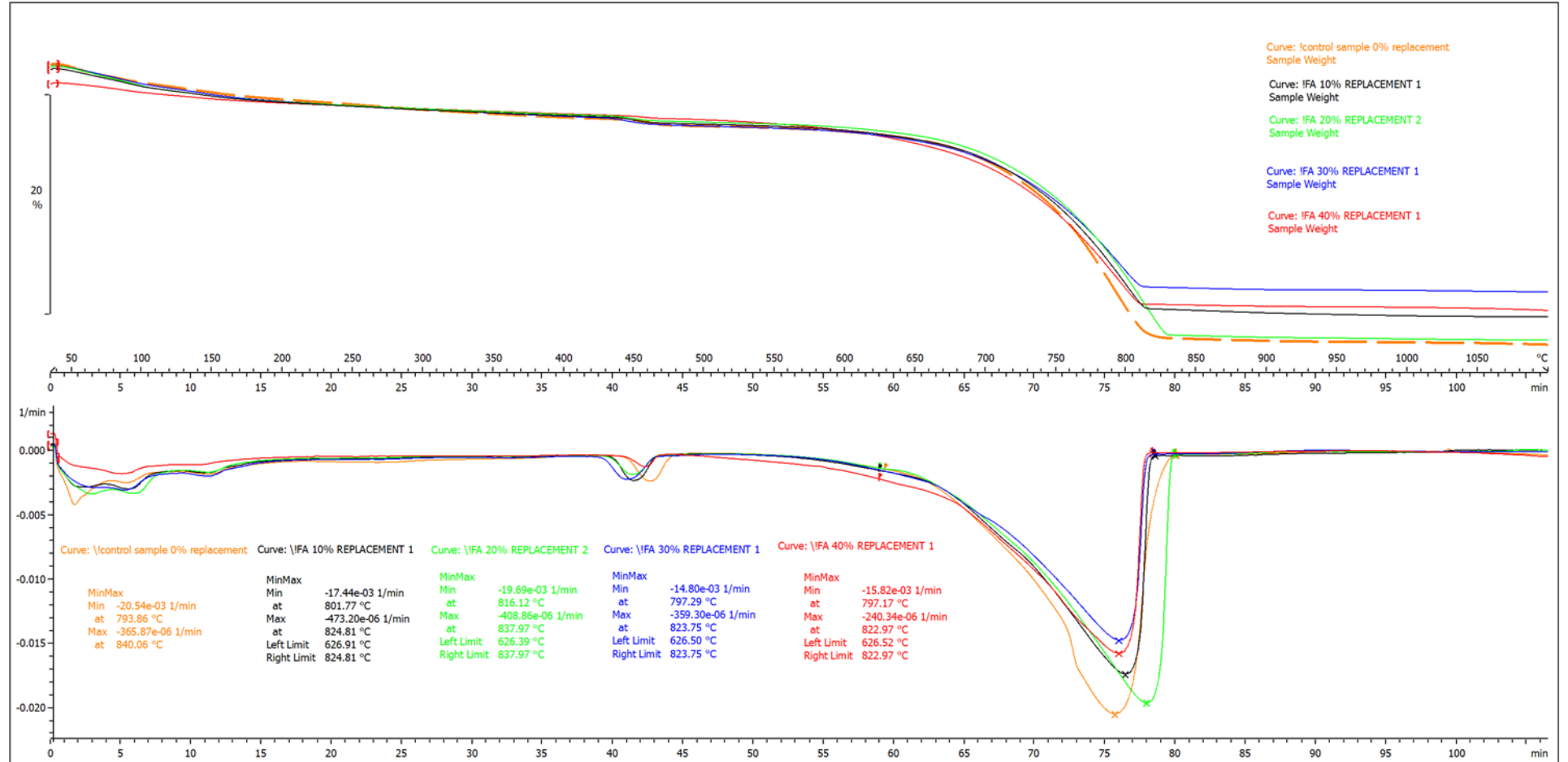
STAR® SW 14.00

Figure 16: TGA of POFA SCC at 7 Days

^exo

7 days FA

29.08.2016 00:10:39



METTLER TOLEDO

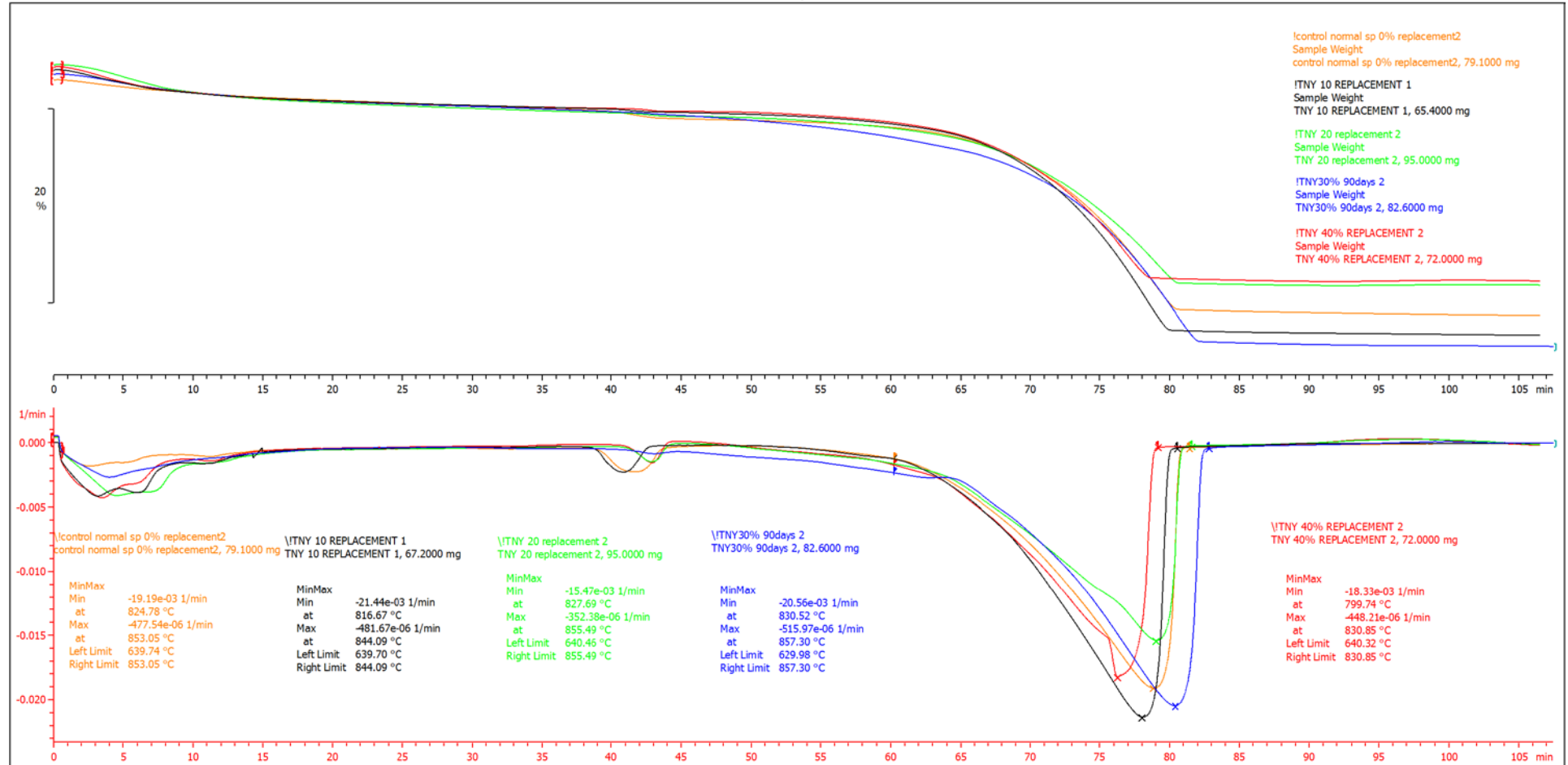
STAR® SW 14.00

Figure 17: TGA of FA SCC at 7 Days

^exo

New 7 day TNY

03.10.2016 09:38:14



METTLER TOLEDO

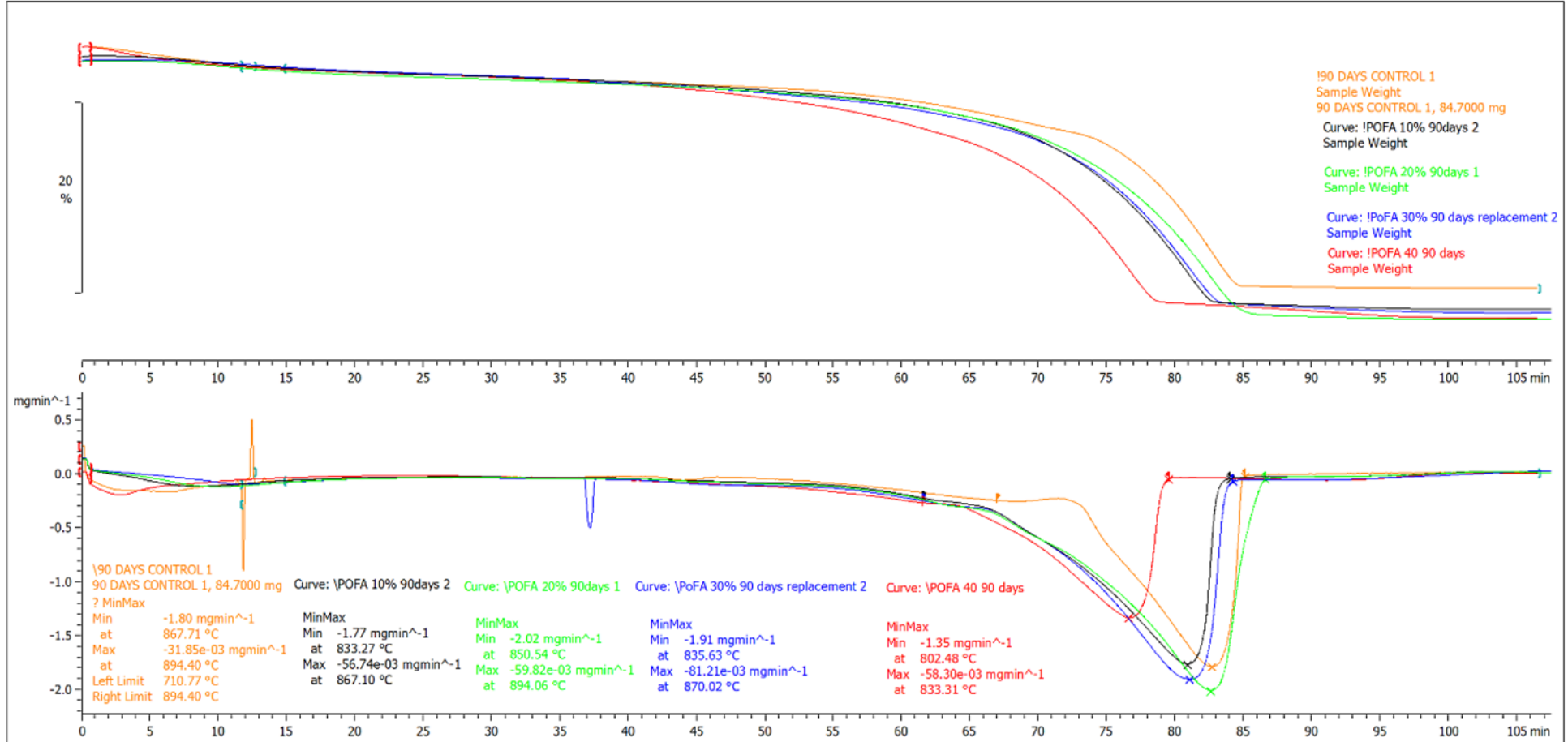
STAR® SW 14.00

Figure 18: TGA of TNY SCC at 7 Days

^exo

90 days POFA

27.08.2016 19:27:29



METTLER TOLEDO

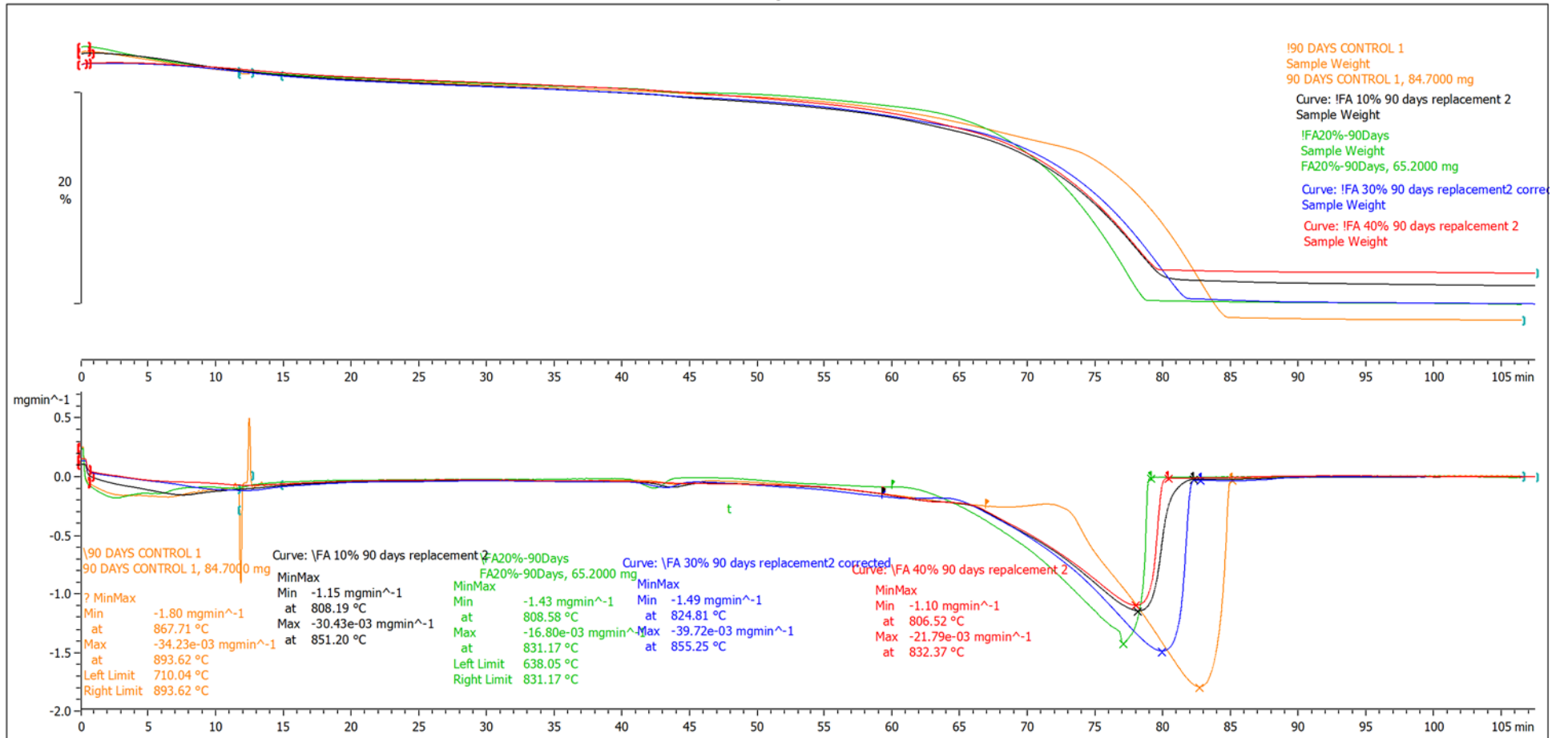
STAR[®] SW 14.00

Figure 19: TGA of POFA SCC at 90 Days

^exo

90 days FA

27.08.2016 21:46:45



METTLER TOLEDO

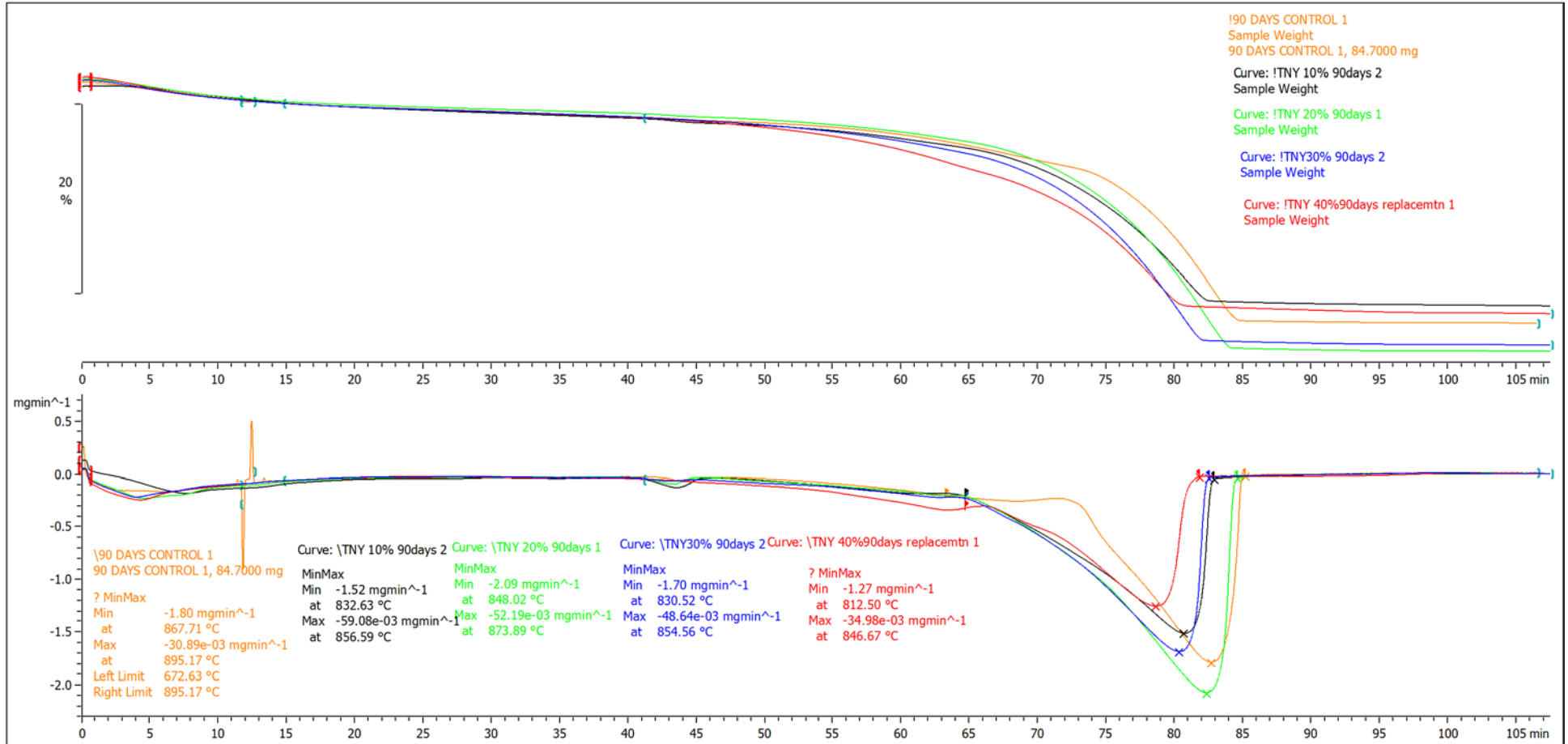
STAR[®] SW 14.00

Figure 20: TGA of FA SCC at 90 Days

^exo

90 days TNY

27.08.2016 19:02:51



METTLER TOLEDO

STAR[®] SW 14.00

Figure 21: TGA of TNY SCC at 90 Days

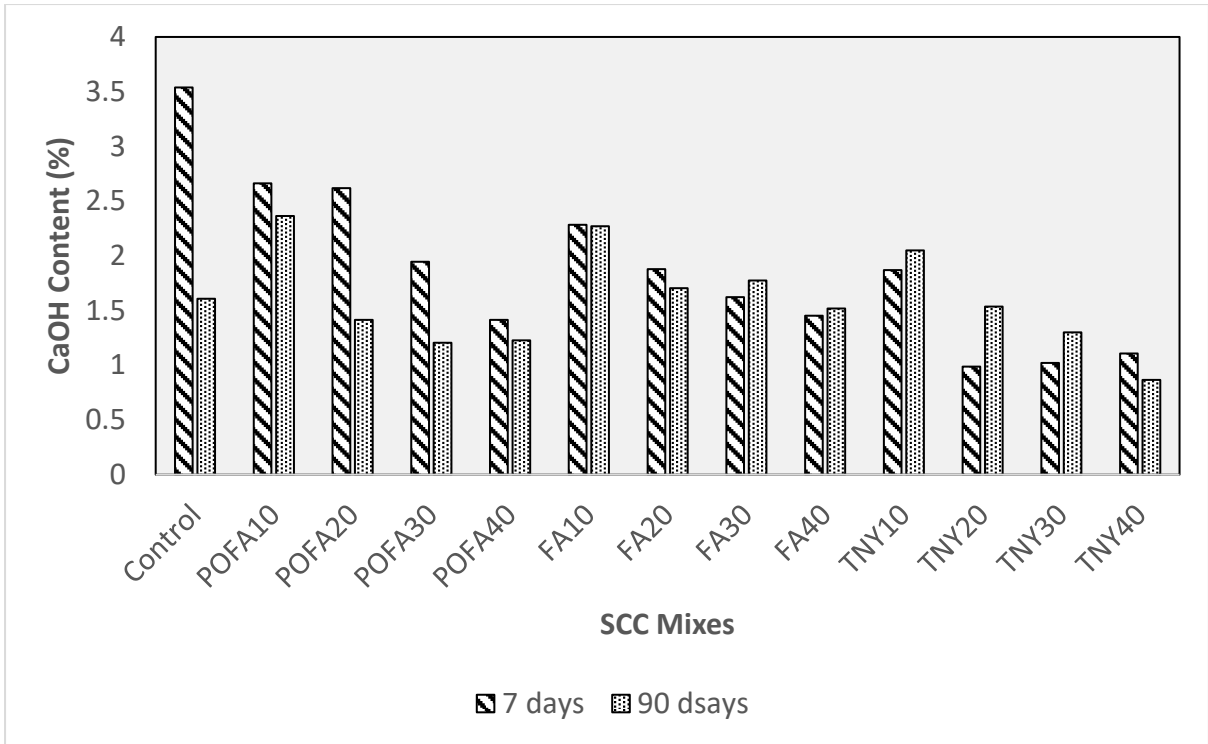


Figure 22: Ca(OH)₂ Content of samples through Thermogravimetric Analysis

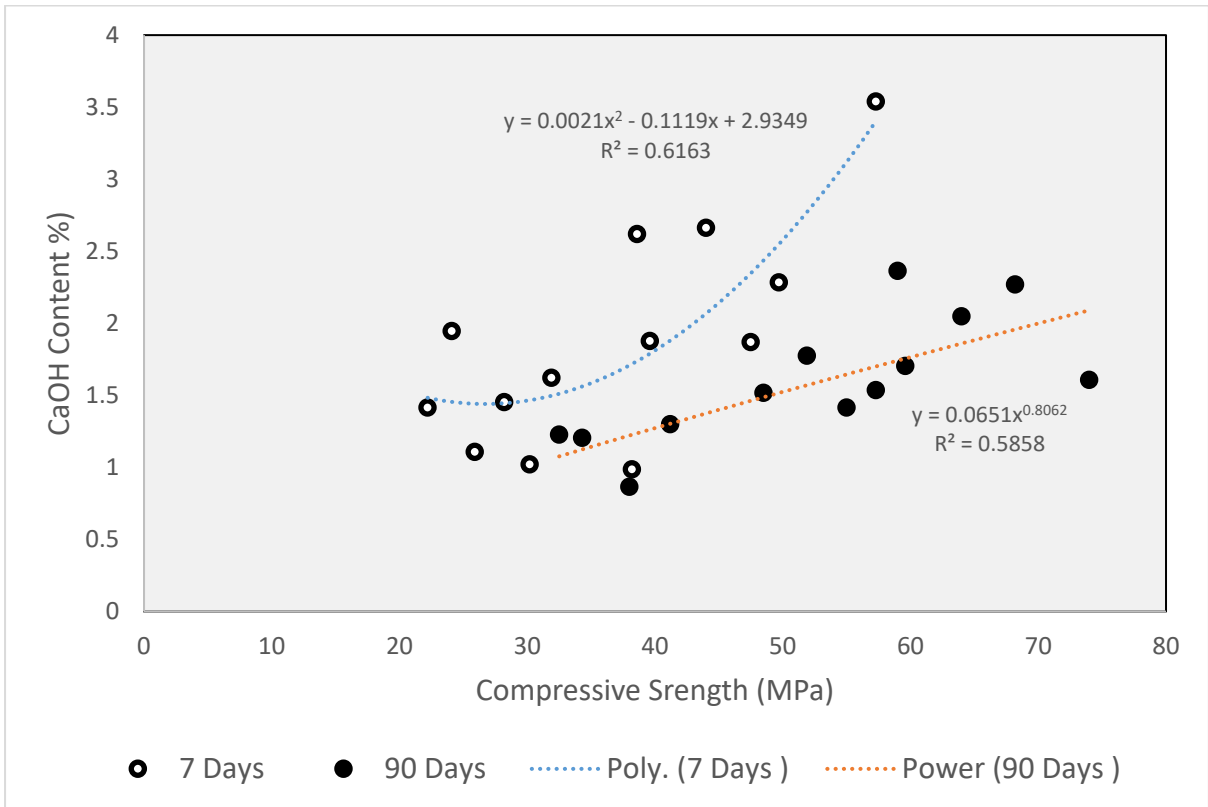


Figure 23: Relationship between Ca(OH)₂ content and Compressive Strength at 7 and 90 days

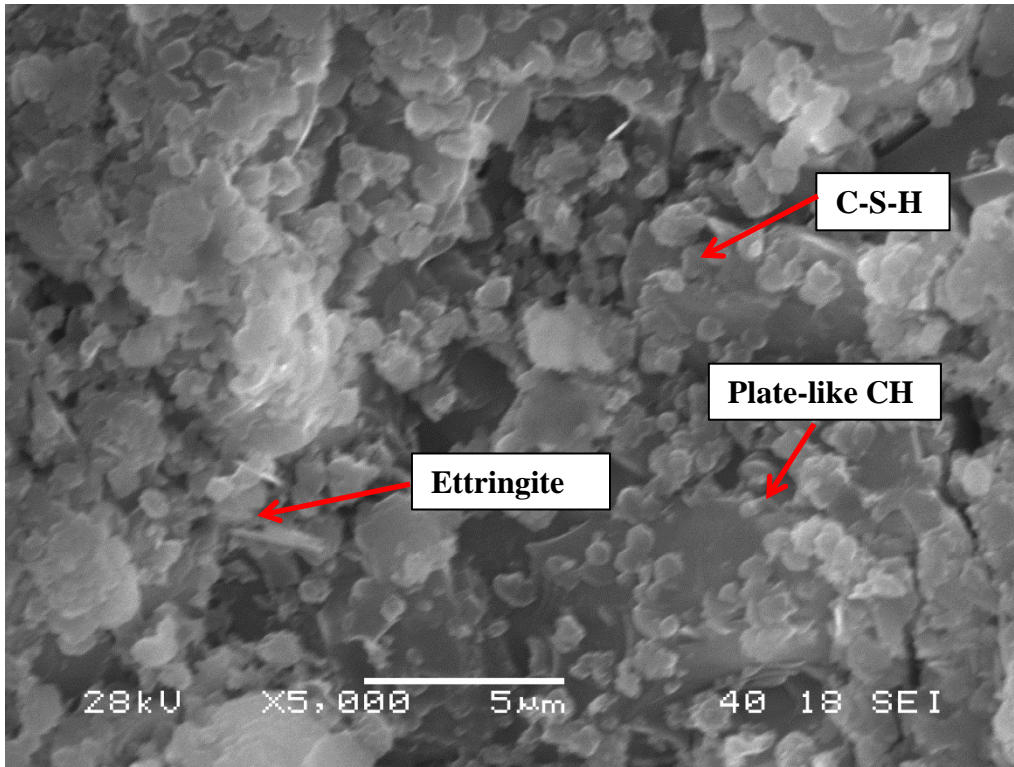


Figure 24: SEM Image for Control SCC at 90 days

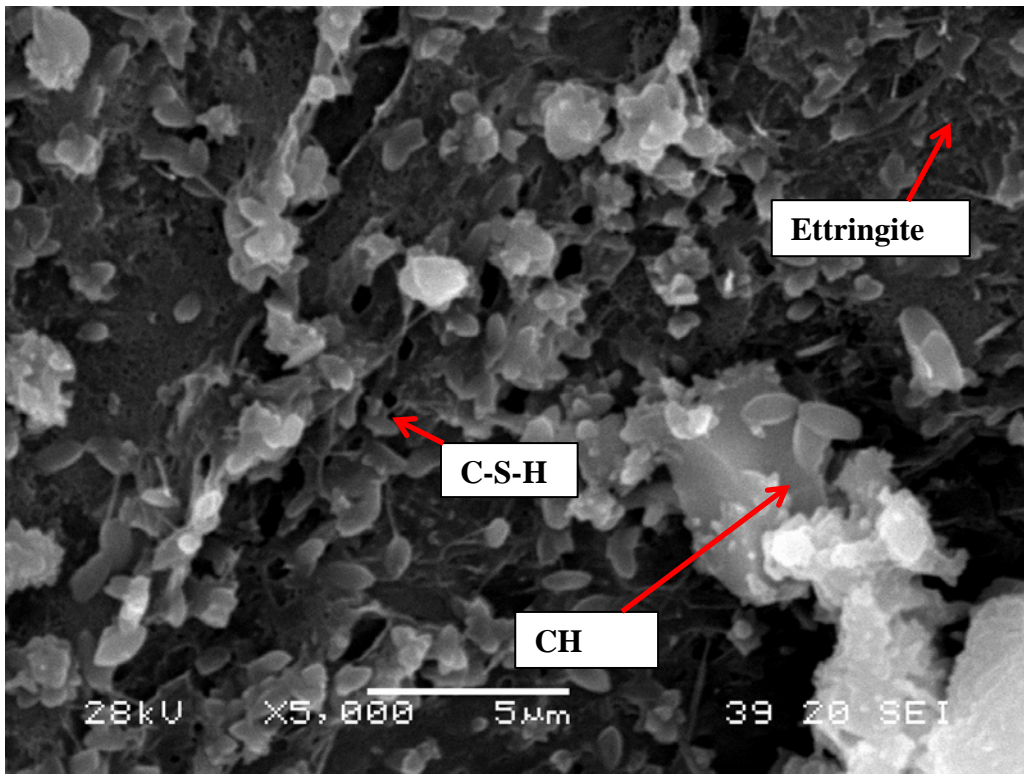


Figure 25: SEM Image for POFA40 at 90 days

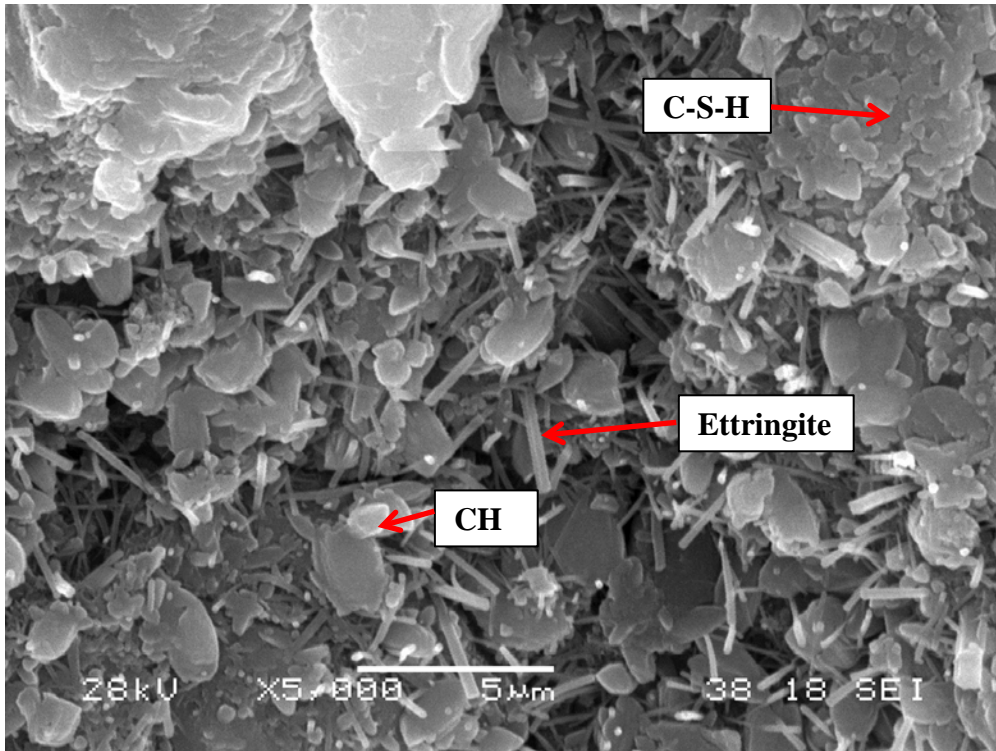


Figure 26: SEM Images for FA40 at 90 days

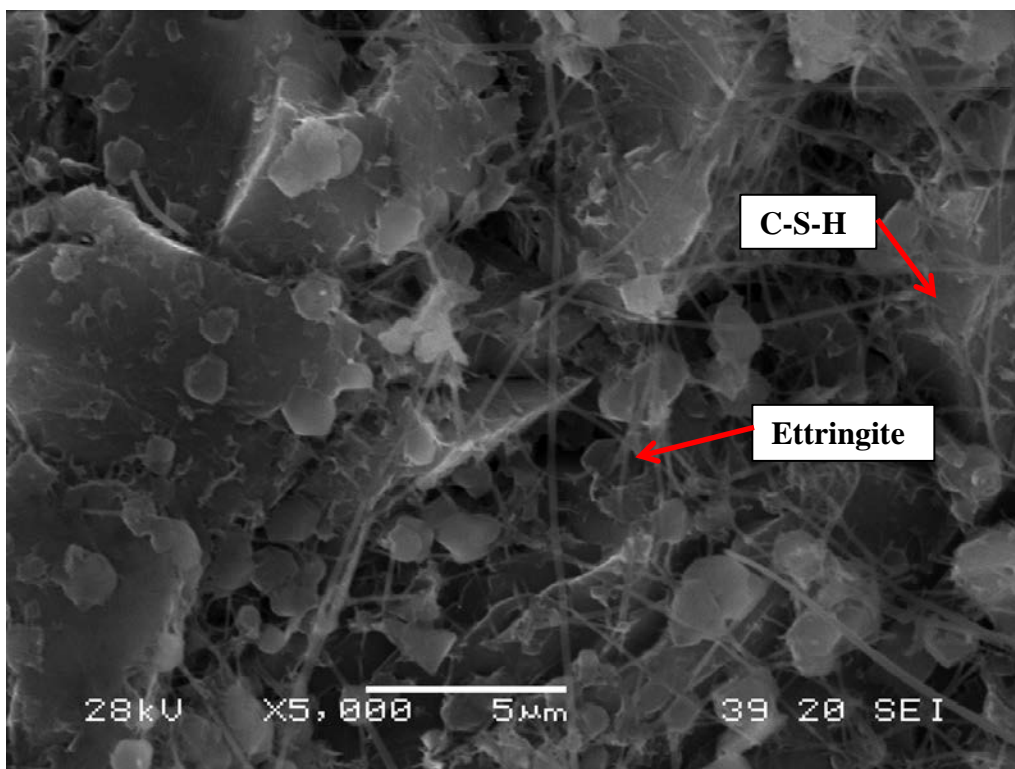


Figure 27: SEM Image for TNY40 at 90 days

TABLE I
PHYSICAL COMPOSITION OF OPC, POFA AND FA

Physical Composition	OPC	POFA	FA
Specific Gravity	3.2	2.2	2.4
Particle retained on 45µm sieve (%)	13	0.3	11.2
Median particle D ₁₀	2.3	1.65	1.85
Median particle D ₅₀	17.2	9.75	13.0
Median particle D ₉₀	49.0	28.8	46.5
Mean diameter	22.1	12.9	19.4
Surface area (cm ² /g)	17,106.4	38,326.4	21,947.7
Soundness (mm)	0.9	2.4	2.2
Strength Activity Index (7 days)	n/a	72	82
Strength Activity Index (28 days)	n/a	81	90

TABLE II
CHEMICAL COMPOSITION OF OPC, POFA AND FA

Chemicals	OPC (%)	POFA (%)	FA (%)	ASTM C150 - Type 1 Requirement for FA (%)
Silicon Dioxide (SiO ₂)	16.29	57.8	55.0	SiO ₂ + Al ₂ O ₃ + Fe ₂ O ₃ >70
Aluminum oxide (Al ₂ O ₃)	4.17	2.3	24.5	
Ferric oxide (Fe ₂ O ₃)	3.51	9.6	7.1	
Calcium oxide (CaO)	68.97	3.60	4.2	<10.0 Class F
Magnesium oxide (MgO)	1.73	1.40	1.95	< 5.0
Sulphur trioxide (SO ₃)		-	0.08	< 5.0
Potassium Oxide K ₂ O	0.99	3.50	3.88	-
TiO ₂ (Titanium Oxide)	-	0.11	2.02	-
Sodium Oxide (Na ₂ O)	0.1	0.56	0.30	<1.5
Loss on Ignition (LOI)	-	20.7	0.32	< 6.0

TABLE III
PHYSICAL, MECHANICAL AND CHEMICAL PROPERTIES OF AGGREGATES

PROPERTIES	Fine Aggregate		Coarse Aggregate
	0 to 600µm (River Sand)	600µm to 5.0mm (Crushed Quarry Dust)	5.0mm to 10.0mm (Crushed Quartz)
Physical Properties			
Maximum Size	600 µm	5mm	10mm
Specific Gravity (SSD)	2.64	2.67	2.62
Moisture Content as received, %	0.7	0.78	0.8
Water Absorption Capacity (24 hrs), %	3.2	1.1	1.4
Bulk Density, Compacted, kg/m ³	1600	1660	1450
Fineness Modulus	1.29	4.29	6.84
Void Ratio	0.65	0.60	0.80
Angularity Number	7	5	12
Mechanical Properties			
Los Angeles Abrasion Value (%)	-	-	18
Aggregate Impact Value (%)	-	-	15
Aggregate Crushing Value (%)	-	-	17
Chemical Properties			
Sulphur trioxide (SO ₃)	0.01	0.01	0.01
Chloride Content	<0.01	<0.01	<0.01

TABLE IV
SP CONTENT FOR ALL SCC MIXES

Mix	SP Content (%)
C	1.10
FA10	0.80
FA20	0.75
FA30	0.66
FA40	0.66
POFA10	1.10
POFA20	1.10
POFA30	1.20
POFA40	1.40
TNY10	1.10
TNY20	1.10
TNY30	1.10
TNY40	1.10

TABLE V
Ca(OH)₂ CONTENT OF SCC SAMPLES

Sample	Ca(OH) ₂ Content (%)	
	7 Days	90 Days
Control	3.54	1.61
POFA10	2.66	2.37
POFA20	2.62	1.42
POFA30	1.95	1.21
POFA40	1.42	1.23
FA10	2.28	2.27
FA20	1.88	1.70
FA30	1.62	1.78
FA40	1.45	1.52
TNY10	1.87	2.05
TNY20	0.99	1.54
TNY30	1.02	1.30
TNY40	1.11	0.87